NASA CR-170608

DEVELOPMENT OF A HgCdTe PHOTOMIXER AND IMPEDANCE MATCHED GaAs FET AMPLIFIER

J.F. Shanley, W.A. Paulauskas, and D.R. Taylor
HONEYWELL INC.
Electro-Optics Operations
2 Forbes Road
Lexington, Massachusetts 02173

TECHNICAL REPORT

Final Report for Period:

4 November 1980 to 1 September 1982

Contract Number: NAS5-26365

Prepared For:

National Aeronautics and Space Administration
Goddard Space Flight Center
Greenbelt Road
Greenbelt, Maryland 20771

DEVELOPMENT OF A HgCdTe PHOTOMIXER AND IMPEDANCE MATCHED GaAs FET AMPLIFIER

J.F. Shanley, W.A. Paulauskas, and D.R. Taylor
HONEYWELL INC.
Electro-Optics Operations
2 Forbes Road
Lexington, Massachusetts 02173

TECHNICAL REPORT

Final Report for Period:

4 November 1980 to 1 September 1982

Contract Number: NAS5-26365

Prepared For:

National Aeronautics and Space Administration
Goddard Space Flight Center
Greenbelt Road
Greenbelt, Maryland 20771

Unclassified

SECURITY CLASSIFICATION OF THIS PAGE (When Data Entered)

REPORT DOCUMENTATION PAGE

READ INSTRUCTIONS BEFORE COMPLETING FORM

1. REPORT NUMBER

2. GOVT ACCESSION NO.

3. RECIPIENT'S CATALOG NUMBER

4. TITLE (and Subtitle)

Development of a HgCdTe Photomixer and Impedance Matched GaAs FET Amplifier

5. TYPE OF REPORT & PERIOD COVERED

Technical (Final)
4/11/80 to 9/1/82

6. PERFORMING ORG. REPORT NUMBER

7. AUTHOR(s)

J. F. Shanley, W. A. Paulauskas, and D. R. Taylor

8. CONTRACT OR GRANT NUMBER(s)

NAS5-26365

9. PERFORMING ORGANIZATION NAME AND ADDRESS

Honeywell Electro-Optics Operations
2 Forbes Road
Lexington, MA 02173

10. PROGRAM ELEMENT, PROJECT, TASK AREA & WORK UNIT NUMBERS

11. CONTROLLING OFFICE NAME AND ADDRESS

National Aeronatuics and Space Administration
Goddard Space Flight Center
Greenbelt Rd., Greenbelt, Maryland 20771

12. REPORT DATE

November 1982

13. NUMBER OF PAGES

56

14. MONITORING AGENCY NAME & ADDRESS(if different from Controlling Office)

15. SECURITY CLASS. (of this report)

Unclassified

15a. DECLASSIFICATION/DOWNGRADING SCHEDULE

16. DISTRIBUTION STATEMENT (of this Report)

17. DISTRIBUTION STATEMENT (of the abstract entered in Block 20, if different from Report)

18. SUPPLEMENTARY NOTES

19. KEY WORDS (Continue on reverse side if necessary and identify by block number)

IR Heterodyne Detector	GaAs FET
Mercury Cadmium Telluride	Cooled Amplifier
p-n Junction Detector	Noise Equivalent Power
High Speed Photodiode	Impedance Matching

20. ABSTRACT (Continue on reverse side if necessary and identify by block number)

This report describes a research program for the development of a 10.6 μm HgCdTe photodiode/GaAs FET amplifier package for use at cryogenic temperatures (77k). The photodiode/amplifier module achieved a NEP/B of 5.7×10^{-20} W/Hz at 2.0 GHz. The heterodyne sensitivity of the HgCdTe photodiode was improved by designing and building a low-noise GaAs FET amplifier operating at 77K. The Johnson noise of the amplifier was reduced at 77K, and thus resulted in an increased photodiode heterodyne sensitivity.

DD FORM 1 JAN 73 1473 EDITION OF 1 NOV 65 IS OBSOLETE

Unclassified

SECURITY CLASSIFICATION OF THIS PAGE (When Data Entered)

PREFACE

This final technical report documents research performed at Honeywell Electro-Optics Operations during the period 4 November 1980 to 1 September 1982 under Contract Number NAS5-26365 with the National Aeronautics and Space Administration. Program technical direction was under the Goddard Space Flight Center, Greenbelt, Maryland. The program Technical Monitor was Dr. Theodore Kostiuk, Code 693.

Technical contributions to the research at Honeywell Electro-Optics Operations were made by Burton Bray, Dave Wolin, and Christopher Flanagan. Special thanks are due to Ms. Donna Borland and Ms. Susan LaFosse for their help in preparing this manuscript.

This report describes a research program for the development of a 10.6μm HgCdTe photodiode/GaAs FET amplifier package for use at cryogenic temperatures (77K). The photodiode/amplifier package achieved a noise equivalent power per unit bandwidth of 5.7×10^{-20} W/Hz at 2.0 GHz. The heterodyne sensitivity of the HgCdTe photodiode was improved by designing and building a low noise GaAs FET amplifier that operated at 77K. The Johnson noise of the amplifier was reduced at 77K (noise of figure of 1.5 dB), and this resulted in an increased photodiode heterodyne sensitivity.

TABLE OF CONTENTS

LIST OF ILLUSTRATIONS

LIST OF ILLUSTRATIONS (continued)

LIST OF TABLES

SECTION 1

INTRODUCTION AND SUMMARY

1.1 Objective

The objective of the "Development of a HgCdTe Photomixer and Impedance Matched GaAs FET Amplifier" program was to develop a HgCdTe photomixer and a low noise GaAs FET amplifier operating at liquid nitrogen temperatures. The efforts of the experimental research were directed towards the development of the technology necessary to fabricate a HgCdTe photodiode/GaAs FET amplifier package which met the following goals:

Photodiode Peak Wavelength:	10.6μm
Photodiode Cutoff Wavlength:	>12.0μm
Effective Heterodyne Quantum Efficiency:	30% at 2.0 GHz without AR coating
Photoactive Area:	$1.8 \times 10^{-4} cm^2$
Operating Temperature:	77K
Amplifier Noise Figure:	≤1.5 dB at 77K
Amplifier Flatness:	±0.5 dB Goal
Amplifier Gain:	≥10 dB
Amplifier Bandwidth:	500 MHz to 3.0 GHz
Operating Temperature:	77K
Size (excluding the active bias circuitry which will be contained in a separate chassis outside the dewar):	2 x 2 x 1" Max.

The major emphasis of the program was to develop a GaAs FET amplifier with a low noise figure (1.5 dB), and a bandwidth

of 500 MHz to 3000 MHz. Previous to this work, the heterodyne performance of 10.6μm HgCdTe photodiodes was limited by the Johnson noise (noise figure of 2.6 dB at 300K) contributed by the amplifier.[1-1] Reduction of the amplifier noise figure from 2.6 dB to 1.5 dB not only results in an improved heterodyne sensitivity, but also the amount of local oscillator (LO) power required for shot noise limited operation is reduced.

For many infrared heterodyne spectroscopy applications which utilize tunable diode lasers (TDL) as the local oscillator, the signal-to-noise ratio can be maximized if the Johnson noise of the amplifier is reduced. The power output of the TDL is low compared to that associated with the CO_2 laser; therefore, the TDL can more easily drive the HgCdTe photodiode into the shot noise limited regime if the amplifier noise figure is limited to values of approximately 1.5 dB.[1-3]

1.2 Technical Approach

The technical approach for developing the technology required for obtaining a low noise HgCdTe photodiode/GaAs FET amplifier package operating at 77K was structured around five primary tasks. They were:

1. Fabricate wide bandwidth 10.6μm n^+-n^--p $Hg_{0.8}Cd_{0.2}Te$ photodiodes using the mercury diffusion process. Design a photodiode microwave mounting structure and dewar that is compatible with the GaAs FET amplifier.

2. Design and build a GaAs FET amplifier operating at 77K. Reduce the GaAs FET amplifier operating temperature from 300K to 77K in order to obtain a

substantial decrease in the amplifier Johnson noise. The amplifier must have a bandwidth of 500 MHz to 3000 MHz, a gain of 10 dB or greater, and a noise figure of 1.5 dB.

3. Characterize the low noise amplifier to show that it meets the gain, noise figure, bandwidth, and operating temperature design goals.

4. Select and characterize an n^+-n^--p HgCdTe photodiode for integration with the GaAs FET amplifier in a bottom looking liquid nitrogen dewar.

5. Completely characterize the heterodyne performance of the photodiode/amplifier package.

1.3 Summary of Results

A low noise GaAs FET amplifier capable of operating at 77K was designed and built during the program. The measured characteristics of the amplifier were:

Operating Temperature:	77K
Gain:	25 dB
Gain Flatness	± 0.5 dB
Noise Figure:	1.6 dB
1 dB Compression Point:	+10 dBm (300K)
Bandwidth:	300 to 3200 MHz
Power.	+15 VDC @ 60 mA

The wide bandwidth 10.6μm n^+-n^--p $Hg_{0.8}Cd_{0.2}Te$ photodiode was fabricated by the mercury diffusion process, and characterization measurements were performed to select the best photodiode for integration with the amplifier. The photodiode that was selected had the following characteristics:

Detector Bandwidth:	>2.0 GHz
DC Quantum Efficiency (10.6μm):	60%
Spectral Peak:	12.0μm
Responsivity (R_λ)(10.6μm):	5.12 A/W
D* (10.6μm, 10 KHz, 1 Hz):	1.3×10^{10} cmHz$^{1/2}$/W
R_S - Series Resistance:	<20Ω
R_O - Zero Bias Resistance:	1500Ω

The photodiode/amplifier package was mounted in a specially designed bottom looking liquid nitrogen dewar. The hold time of the dewar was measured to be approximately 12 hours, and the dewar had a barium fluoride window.

The heterodyne performance of the HgCdTe photodiode/amplifier package was measured at 77K to be:

Heterodyne Bandwidth:	> 2.0 GHz
Noise Equivalent Power (NEP/B) at 2.0 GHz:	5.7×10^{-20} W/Hz
Effective Heterodyne Quantum Efficiency:	32.8% at 2.0 GHz
Incident LO Power:	0.39 mW
Detector Bias Voltage:	0.93 Volts

SECTION 2

n^+-n^--p PHOTODIODE DEVICE DEVELOPMENT

2.1 n^+-n^--p Photodiode Fabrication

Planar processing techniques were used to fabricate the n^- junctions (active area is 1.8×10^{-4} cm^2) on a substrate of p-type ($N_A \approx 1.0 \times 10^{17}$ cm^{-3}) $Hg_{0.8}Cd_{0.2}Te$.[2-1, 2-2] The low carrier concentration n^- layer ($N_D \approx 5.0 \times 10^{14} cm^{-3}$) was achieved by a two temperature anneal in a mercury atmosphere. A shallow n^+ layer ($N_D \approx 1.0 \times 10^{18}$ cm^{-3}) was applied to the surface of the n^- region in order to limit the device series resistance to values of approximately 10 to 20 ohms. Indium contact pads were evaporated on the n-type layer, and gold was plated on the back surface to form an ohmic contact. Figure 2-1 illustrates the procedures involved in fabricating the n^+-n^--p photodiodes.

Upon completion of the fabricaton procedure, the (Hg,Cd)Te wafer is diced into chips containing twelve photodiodes, and then affixed to a specially designed microwave mounting structure.

2.2 Junction Process Development

A mercury diffusion process was used to form the n^- junctions on a substrate of p-type $Hg_{0.8}Cd_{0.2}Te$.[2-3] The substrate was sliced from an ingot of material that was grown by the quench/anneal technique, and was p-type due to a nonstoichiometric defect, presumably mercury vacancies. To achieve wide bandwidth n^+-n^--p photodiodes the p-type substrate, containing 0.6×10^{17} - 1.0×10^{17} cm^{-3} non-stoichiometric defects, must convert upon annealing in a mercury

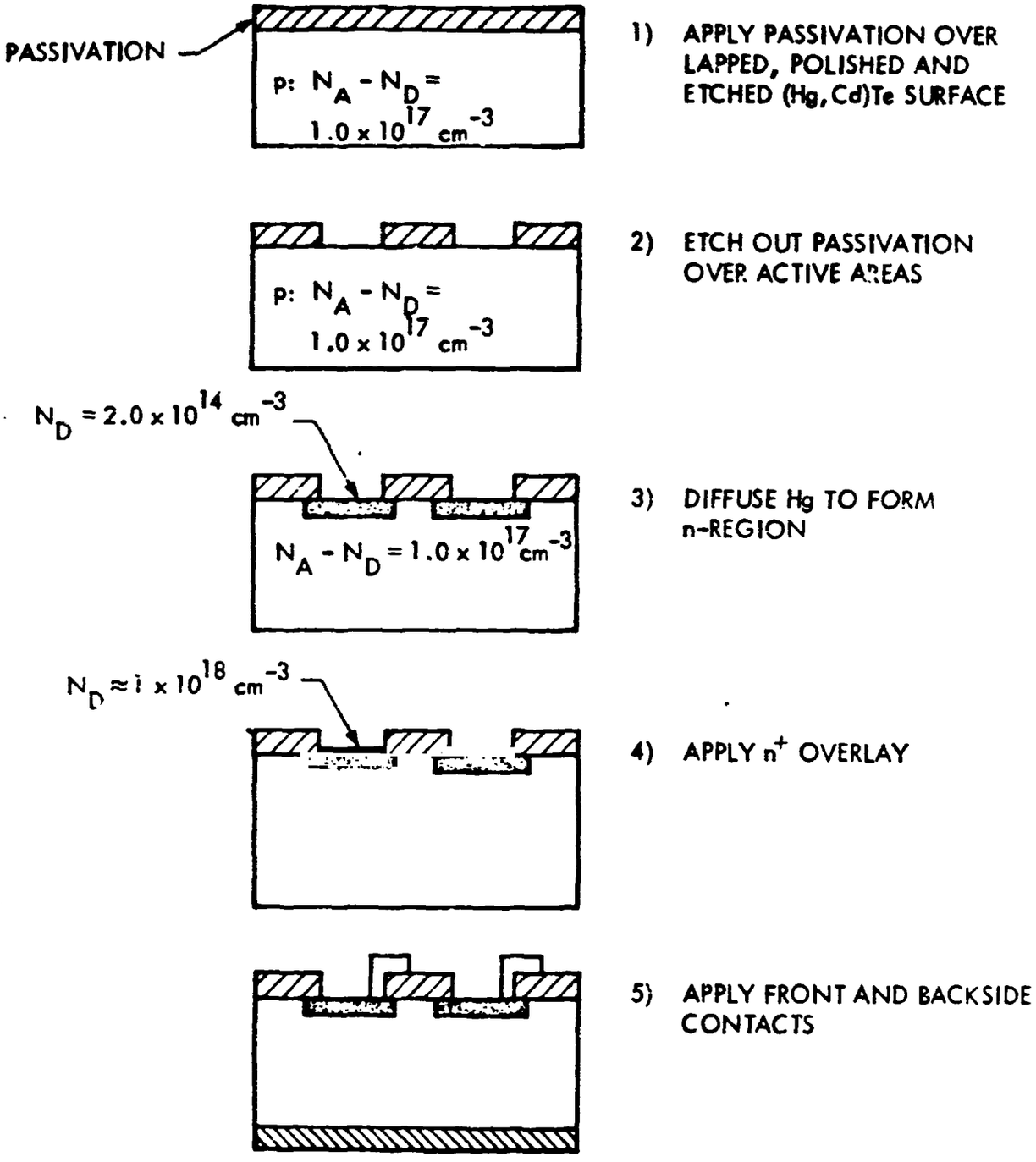

Figure 2-1 Mercury Diffusion Process for the n^+-n^--p Photodiode.

atmosphere to an n^- layer containing a net donor concentration of approximately 5.0×10^{14} cm^{-3}. Under these conditions, mercury diffuses into the substrate annihilating the mercury vacancies, thereby allowing the residual n-type impurities already present in the solid to predominate.[2-4]

The diffusion of mercury into p-type (Hg,Cd)Te can be described by Fick's law of diffusion[2-5]

$$D(T) = D_o \exp\left(-\frac{\Delta E}{kT}\right),$$

where D(T) is the diffusion coefficient, D_o is the frequency factor, ΔE is the activation energy, k is Boltzmann's constant, and T is the absolute temperature. The values of the above parameters are determined by the physiochemical properties of the medium in which the diffusion is taking place and by those of the diffusion species.

The optimum junction design for wide bandwidth devices requires that the thickness of the n^- layer be equal to $1/\alpha$ centimeters, where α is the absorption coefficient for 10.6 micrometer radiation in (Hg,Cd)Te. To fabricate diodes with the otpimum geometry, it is necessary to determine the relationship between junction depth (n^- layer thickness) and diffusion schedule. The junction depth X_J is related to the diffusion coefficient and the time t by the following expression:

$$X_J = 2\sqrt{D(T)\ t}.$$

Figure 2-2 presents a graph of the junction depth versus diffusion time, with temperature as a parameter. The junction

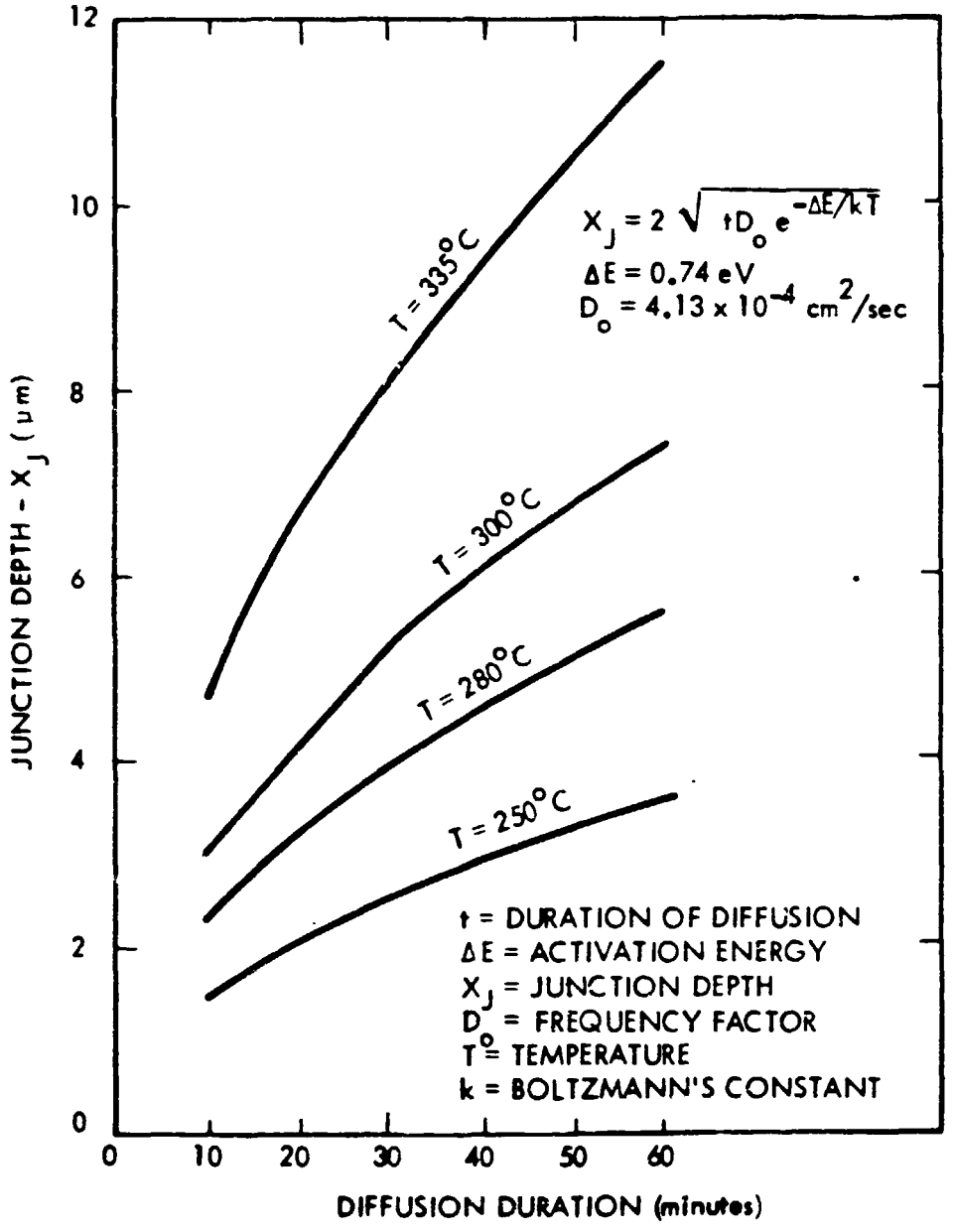

Figure 2-2 Junction Depth Versus Diffusion Time with Temperature as a Parameter.

depths presented in Figure 2-2 were calculated by using an activation energy of 0.74 eV and a frequency factor of $4.13 \times 10^{14} cm^2/s$.

The junction depths obtained by the mercury diffusion process were estimated to be approximately 4.0 to 5.0 micrometers; this value is consistent with $1/\alpha$.[2-6] It is noted from Figure 2-2 that several different diffusion schedules can be used to obtain this particular junction depth.

2.3 Photodiode Microwave Mounting Structure

The heterodyne frequency response of the $Hg_{1-x}Cd_xTe$ photodiode is directly influenced by the parasitic impedance of the diode mounting structure. To isolate the diode high frequency response, it is necessary to minimize the effects introduced by the external parasitic impedance. The photodiode chip is mounted in a flatpack with very low parasitic capacitance and inductance over the frequency range from 1 MHz to 4.0 GHz. Gold ribbon, 0.0015 inch by 0.0007 inch is used to make the electrical connection between the photodiode's n^+ region and the flatpack's beam lead. The ground plane of the flatpack was electrically connected to the p-region of the photodiode through the use of a conductive epoxy.

The photodiode flatpack is epoxied to a copper assembly which is mounted on the cold finger of the liquid nitrogen dewar. A thermally conductive epoxy is used in order to insure that the photodiode is maintained at a temperature of 77K. The copper assembly is machined to a wedge geometry, and the plane of the top surface of the photodiode is at a 12^o angle with respect to the surface of the cold finger. The wedge geometry is used to eliminate reflected radiation.

The n^+-p-p^+ $Hg_{0.8}Cd_{0.2}Te$ photodiode is connected to a DC bias tee with a 50 Ω transmission line and SMA RF connector. The RF output port of the DC bias tee is connected to the RF input section of the GaAs FET amplifier. The DC port of the bias tee is connected to the SMA connector labeled "Bias" located on the dewar wall. The RF output port of the GaAs FET amplifier is connected to the SMA connector on the dewar wall labeled "Out". Power is supplied to the GaAs FET amplifier through an SMA connector on the vacuum side of the dewar wall which is labeled "+15" . The voltage regulator is connected to the GaAs FET amplifier. The amplifier operates on a bias voltage of +8 volts at 1.5mA in order to achieve 25 dB of gain at 77K. The amplifier power is provided by a voltage regulator which requies +15 volts and 60mA of external electrical power. Power must be supplied to the amplifier only at 77K, damage will occur if the amplifier is operated at other temperatures.

In summary, the SMA connectors located on the liquid nitrogen dewar wall perform the following functions:

CONNECTOR LABEL	FUNCTION
BIAS	Reverse bias the photodiode (0 to +1.5 Volts).
OUT	Amplified RF output signal (300 to 3200 MHz).
+15	Voltage Regulator Power (+15 Volts, 60 mA).

Finally Figure 2-3 is a photograph and Figure 2-4 is a schematic diagram showing the location of the photodiode, bias T, voltage regulator and GaAs FET amplifier. It might be noted that the photodiode mounting assembly is seated on a 0.5 inch diameter cold finger which extends 0.75 inches from the base on which the GaAs FET is mounted; the entire base is held at a temperature of 77K. The bias T and voltage regulator are suspended in the vacuum space, and neither cooled to 77K.

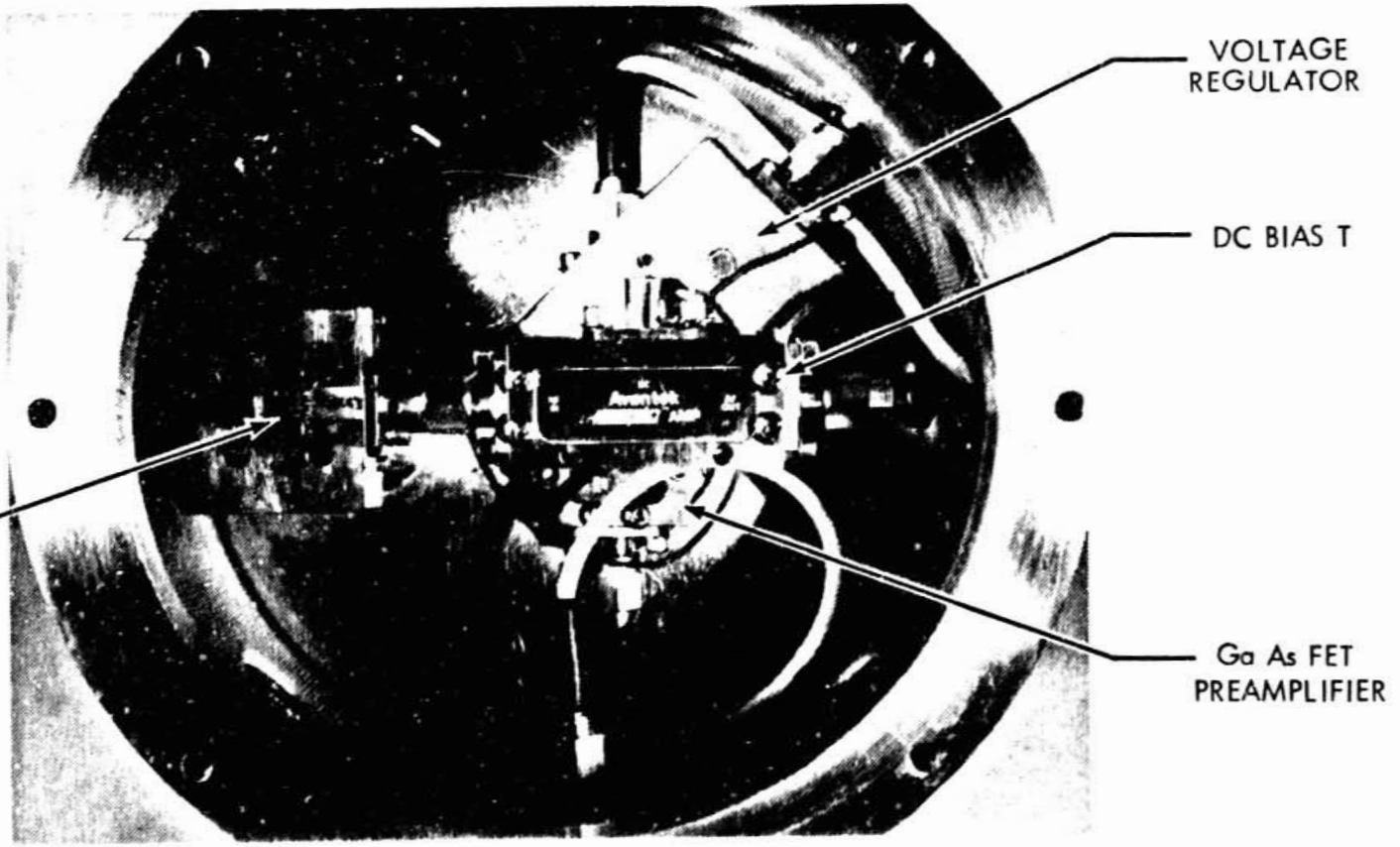

Figure 2-3 Photograph of the Photomixer/GaAs FET Amplifier Mounting Configuration.

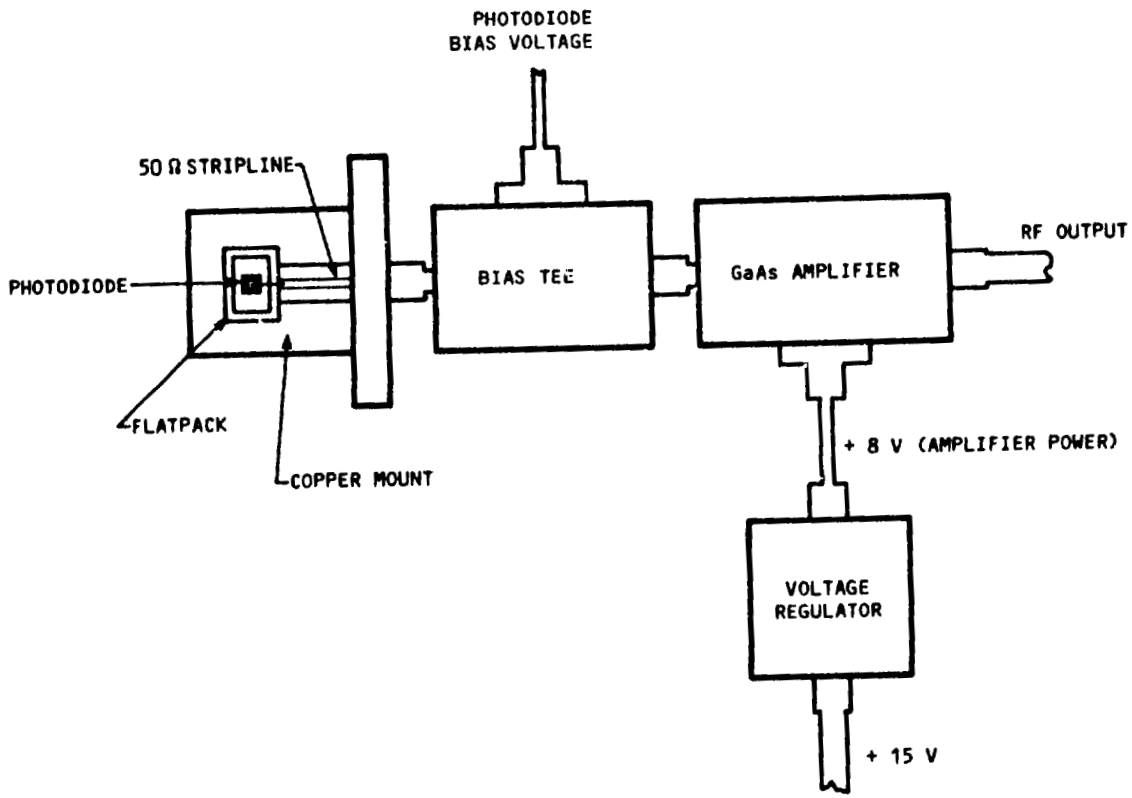

Figure 2-4. Block diagram of the Photodiode/GaAs FET Amplifier Module.

2.4 Dewar

A bottom looking liquid nitrogen dewar was designed and built by International Cryogenics, Inc., of Indianapolis, Indiana. The dewar has a one (1) liter liquid nitrogen capacity, and the entire base is maintained at 77K. A schematic diagram of the LN_2 dewar is presented in Figure 2-5. A 0.5 inch diameter by 0.75 inch length cold finger extends from the base and was used for mounting the photodiode microwave assembly.The bottom flange of the dewar contains a barium fluoride window mounted at 12° to the surface of the cold finger. The center line of the photodiode is postioned to coincide with the center of the barium fluoride window.

Liquid nitrogen hold times of approximately 12 hours were obtained under full heterodyne operating conditions.

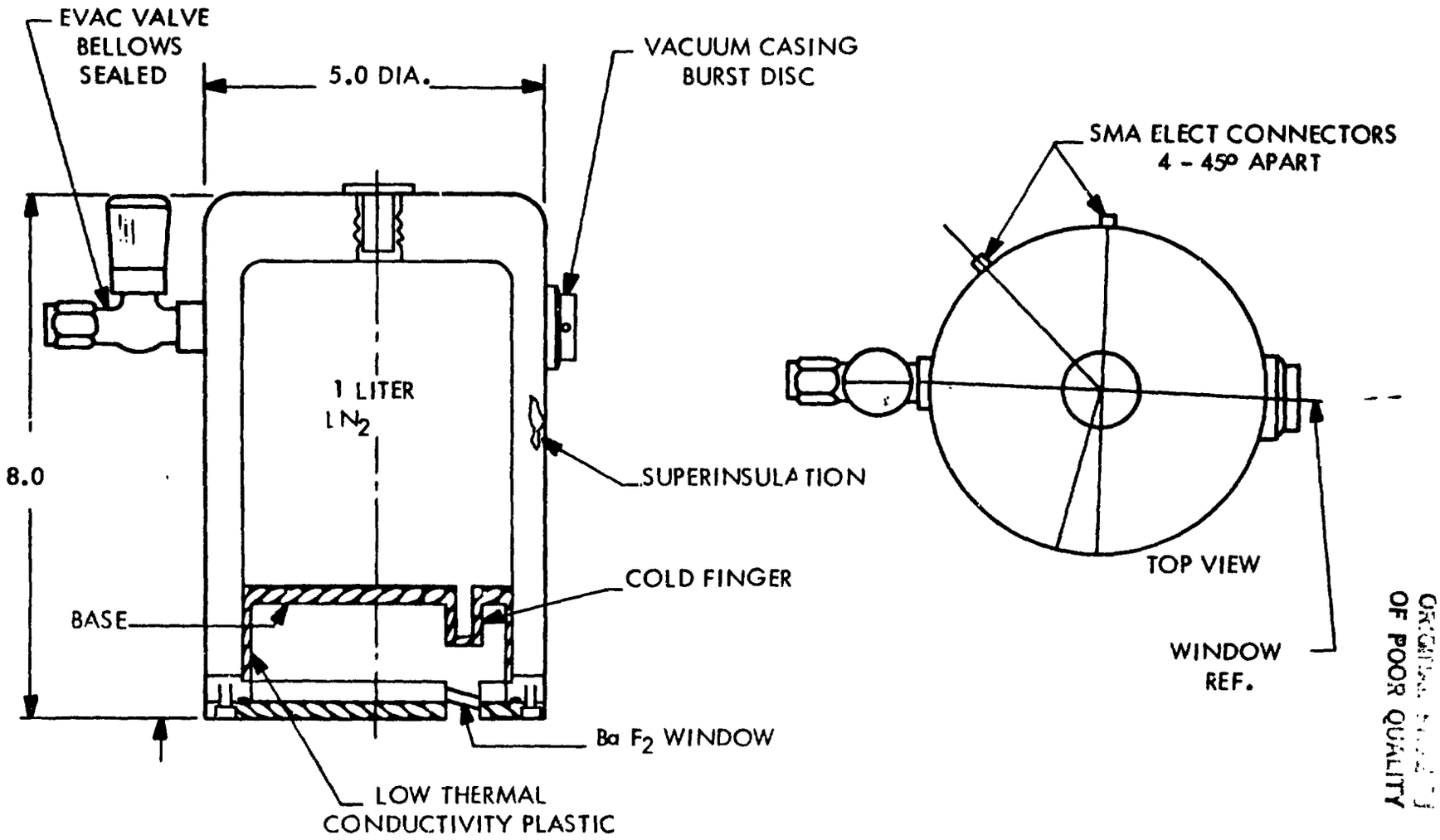

Figure 2-5 Schematic Diagram of the LN_2 Dewar.

SECTION 3

GaAs FET AMPLIFIER DESIGN

The design and construction of the low noise GaAs FET amplifier is discussed in this section. The amplifier was designed to operate at 77K and to have a bandwidth of 500 to 3000 MHz, and a noise figure of 1.5 dB.

The noise figure of the amplifier is of fundamental importance for infrared heterodyne applications using high speed n^+-n^--p $Hg_{0.8}Cd_{0.2}Te$ photodetectors. The Johnson noise contribution of the amplifier, in many instances, can limit the heterodyne performance of the $Hg_{1-x}Cd_xTe$ photodiode. Large amounts of local oscillator (LO) power may be required to overcome the noise contributed by the preamplifier. The CO_2 laser is used as the local oscillator in many infrared heterodyne applications since it is capable of providing sufficient LO power to surmount the amplifier noise. However, the tunable diode laser (TDL) with much less total output power than the CO_2 laser, is increasingly being used as an LO because of its wide frequency tunability. The need to reduce the noise contributed by the amplifier is critical for the successful use of the TDL. Therefore, the goal of this effort was to design and build a wide bandwidth amplifier using GaAs FET's cooled to 77K in order to obtain a noise figure of 1.5 dB.[3-1] Comparable room temperature (300K) amplifiers operating over the 500 to 3000 MHz frequency region have noise figures of approximately 2.5 dB to 4.0 dB.

The initial approach to the design of the GaAs FET preamplifier considered microwave matching the impedance of the

RF input section of the amplifier to the impedance of the $Hg_{0.8}Cd_{0.2}Te$ photodiode. However, network analyzer measurements performed on the photodoiode as a function of detector bias voltage and incident CO_2 laser LO power revealed that the photodiode impedance had a VSWR close to 2:1 over the 500 MHz to 2000 MHz frequency range. The details of these measurements are discussed in Section 6.1. Since the photodiode VSWR was approximately 2:1, it was decided that the RF input impedance of the amplifier could be designed to be 50 ohms. No microwave matching was necessary.

3.1 Low Noise Amplifier Design

The low noise amplifier consists of two gain modules.[3-1,3-2,3-3,3-4] Each gain module is a balanced GaAs FET amplifier using interdigital (Lang) couplers Wide band performance is achieved by:

(1) Utilizing a unique approach of combining two low noise similar GaAs FETs in parallel. A schematic diagram of the wideband low noise amplifier is presented in Figure 3-1. The parallel combination optimum noise source impedance is considerably lower than that of the single FET in the 500-3000 MHz band, see Figure 3-2 , while the optimum noise figure remains unchanged. This enables the use of a single element (inductors) for wide band noise matching. Also, the S_{21} of the parallel combination is increased by about 2.5 to 3 dB thereby reducing the second stage noise figure contribution to the overall noise figure. The dynamic range is doubled.

(2) Using a six strip overcoupled wide band interdigitial (Lang) coupler instead of the conventional four strip three dB coupler.

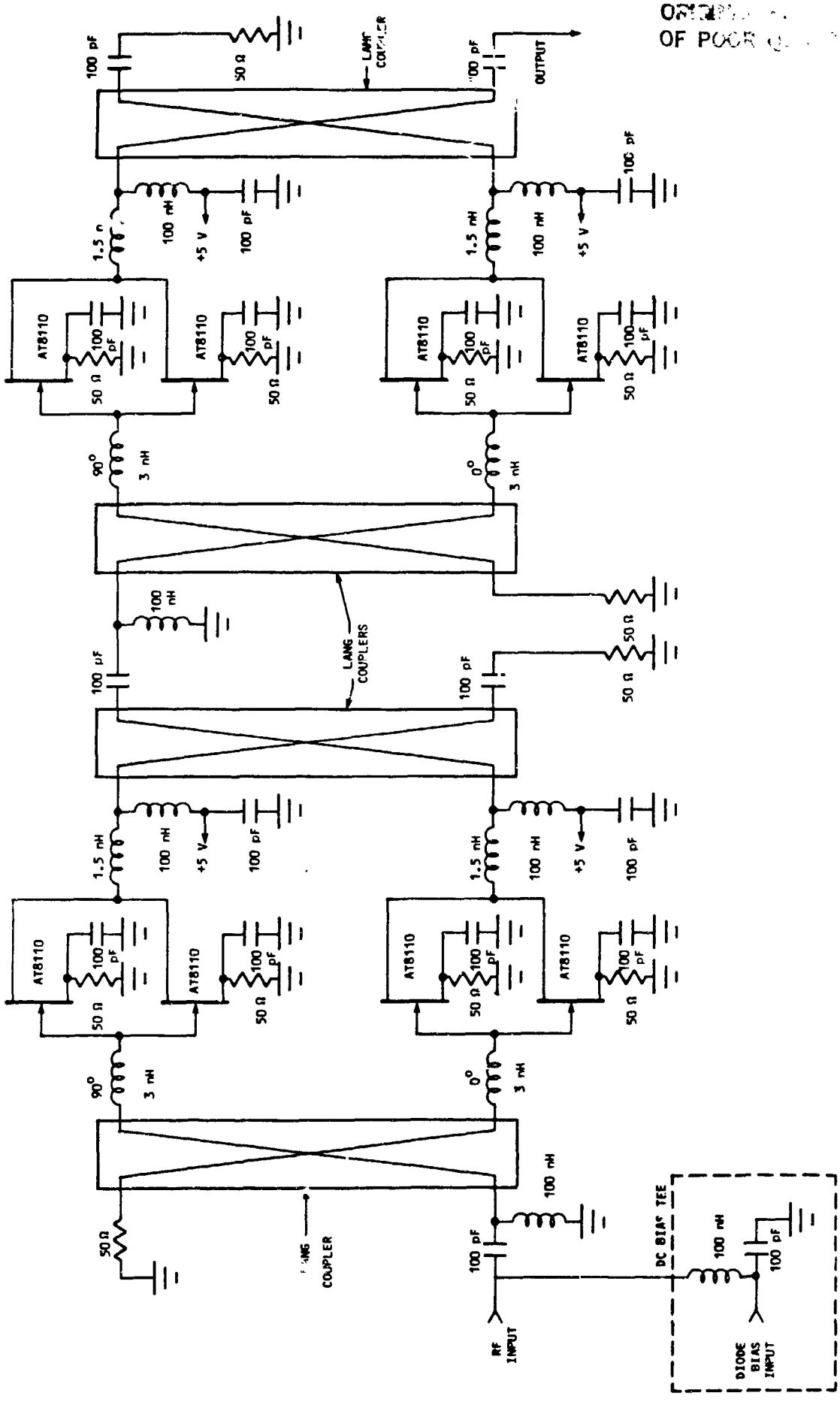

Figure 3-1 Circuit Diagram for the Low Noise GaAs FET Amplifier.

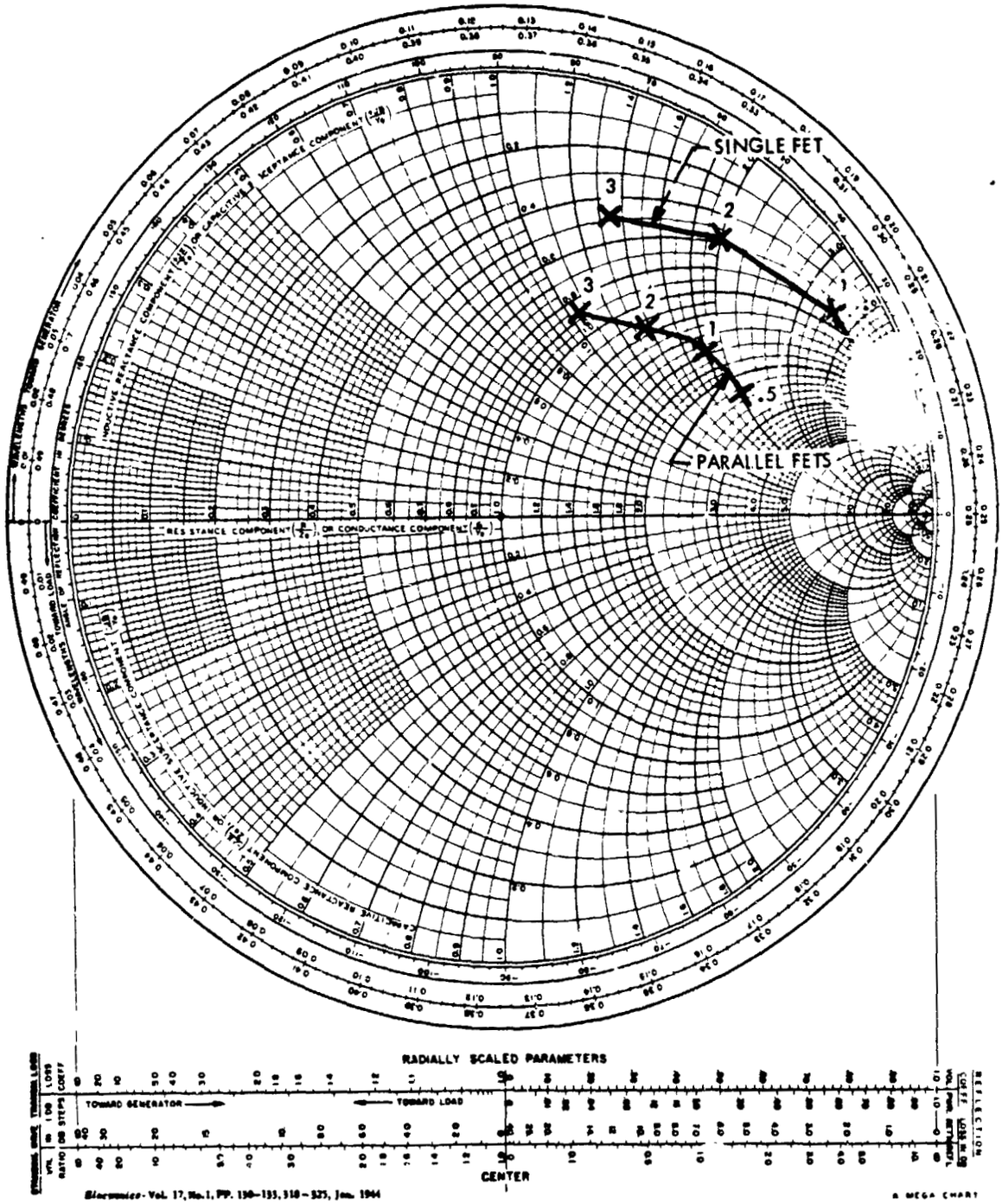

Figure 3-2 Optimum Noise Source Impedance for Single and Parallel Combination FETs.

The amplifier is a two stage balanced design. Both of the balanced stages are identical except the input stage can also incorporate a bias T for supplying the bias voltage to the photodiode. The amplifier circuit diagram illustrated in Figure 3-1 shows the bias T as an integral part of the amplifier. However, for this program the bias T was built in a separate package and connected to the RF input section of the amplifier. There is no reason to have the bias T in a separate package. The amplifier, bias T, and voltage regulator were built in modules because it was less complicated to trouble-shoot the individual components. In addition, the voltage regulator must be in a module because it cannot be cooled to 77K due to carrier freeze out (see Section 3.2). Any future cooled low noise amplifiers that will be built will have an integral bias T, but the voltage regulator will still be in an individual module. More developmental work is required in order to construct a voltage regulator capable of operating at 77K.

The RF input is fed to a six strip interdigital coupler (also known as a Lang coupler). Normal interdigital couplers use four strips and they cover a nominal one octave frequency range. A six strip coupler uses overcoupled design and covers a nominally three octave frequency range. The input signals are split into two equal amplitude 90^{o} quadrature signals at the two output ports of the coupler. As long as the load impedances at the two output ports are identical, power reflected at the output ports are identical, power reflected at the output ports arrives at the input port 180^{o} out of phase, and is thus cancelled at the amplifier input port. The reflected power adds in phase at the terminated port of the coupler and is absorbed in the 50 ohm termination. This design approach results in an amplifier that is simultaneously power matched and noise matched. Care has to be exercised in making the input circuits to the active transistors as identical as physically and electrically possible.

The signals from the input coupler outputs are amplified in a uniquely designed amplifying section. The amplifying section consists of two low noise GaAs FET transistors in parallel. The design feature of the parallel combination is a considerably lower optimum noise source impedance as compared to a single transistor. This lower optimum noise source impedance allows wideband noise matching with a smaller number of elements in the matching network. Smaller number of elements in the input matching network minimizes the resistive losses, and results in an overall lower amplifier noise figure.

The outputs from the amplifying sections are fed into a second quadrature coupler complimentary to the input coupler. Since the two input signals are equal in amplitude but 90° out of phase, they add in phase at the output port and are 180° out of phase at the 50 ohm termination.

The second stage of the balanced amplifier is similar to the input stage except the bias T is deleted.

The amplifier circuit was constructed using thin film techniques. Alumina substrates were formed to a less than 3 microinch finish. Gold conductors and tantalum nitride resistors were deposited in the circuit by PF sputtering. Laser drilling was used to provide holes in the substrates for RF grounding. Substrates were attached to the gold plated Kovar housing by high temperature solder. All wire bonds in the circuit were kept to a minimum length. Finally, the housing was hermetically sealed by electron beam welding. The type of construction described makes this amplifier ideally suited for cooling to extremely low temperatures.

3.2 Voltage Regulator

Initially the GaAs FET amplifier was designed to have an integral voltage regulator and the whole assembly was to be cooled to 77K. Carrier freeze out was observed to occur in the silicon bipolar devices when cooled to 77K. The freeze out effect reduced the regulator output current and voltage which was used to power the GaAs FET's. Consequently, the GaAs FET amplifier performance was severely degraded. To remedy this situation, a new voltage regulator was designed and built to operate in the vacuum space of the dewar.

The electrical circuit that was designed and built for the voltage regulator is presented in Figure 3-3. The input power required by the regulator is +15 VDC and 60 mA. The design utilizes a LM317T which is a state-of-the-art 3 terminal adjustable voltage regulator, in this case configured to deliver +8V volts at a maximum current of 1.5 amperes. The features of the commercially available LM317T include the following; 0.1% line regulation, typically 1.0 volt load regulation, 80 dB ripple rejection, and a rated power dissipation of 15 watts. Additionally, the device is short circuit protected by virtue of internal current limiting, and is also thermal overload protected. Further the unit is heat sunk to the metal enclosure and this provides an extra margin of safety. The voltage output is described by the following expression

$$V_{out} = 1.25\ (1 + R_2/R_1),$$

where R_2 is 1300 Ω and R_1 is 240 Ω .

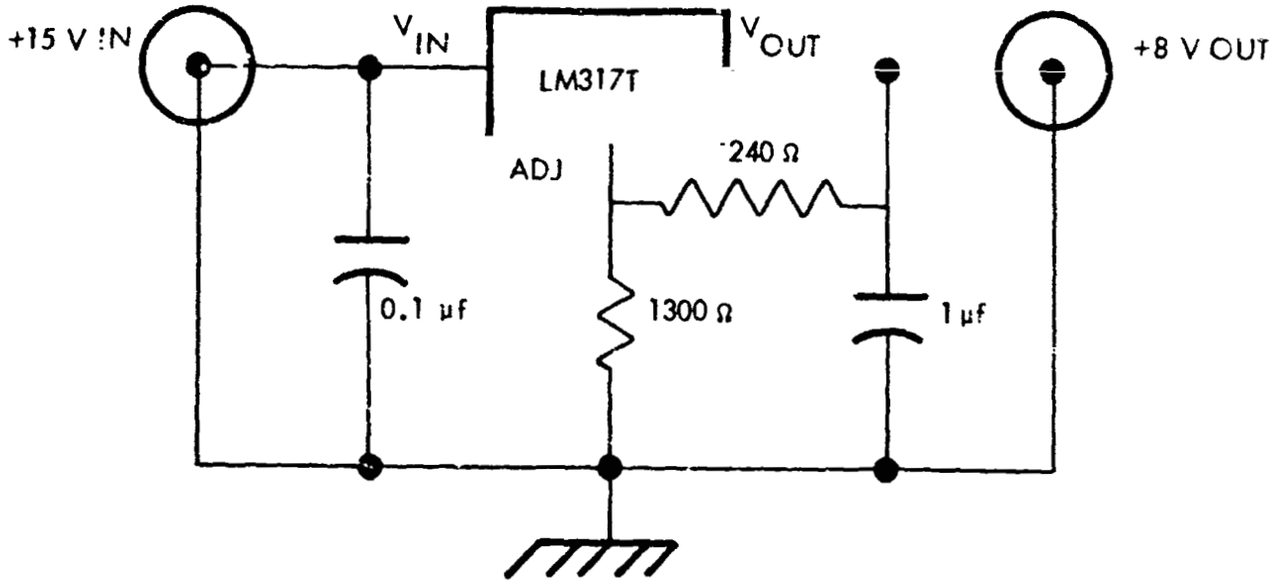

Figure 3-3 Schematic Diagram of the Voltage Regulator for the GaAs FET Amplifier.

SECTION 4

AMPLIFIER CHARACTERIZATION

Gain, noise figure, forward and reverse voltage-standing-wave-ratio VSWR, gain compression, and bandwidth measurements were made with the GaAs FET maintained at 77K and 300K. The results of these measurements are reported in this section.

4.1 Amplifier Gain

The gain of the GaAs FET amplifier was measured in two frequency bands, 200 MHz to 2000 MHz and 2000 MHz to 10,000 MHz, using a HewlettPackard HP8542B computer controlled network analyzer. The amplifier gain at 77K,see Figure 4-1 was approximately 25 dB, while at 300K the gain was about 22 dB, Figure 4-2. Therefore, the gain was observed to increase by approximately 0.135 dB/K. At 77K and 300K the gain was found to be flat over the frequency range from 300 MHz to 3200 MHz. The amplifier high frequency roll off is presented in Figure 4-3, and it is noted that the 3 dB frequency occurs at around 3300 MHz. Similar results were obtained at 300K.

The gain flatness was measured to be approximately $\pm$0.5 dB at 77 and 300K.

4.2 VSWR

The amplifier forward and reverse voltage-standing-wave-ratio's VSWR were measured at 77K and 300K using the HP8542B

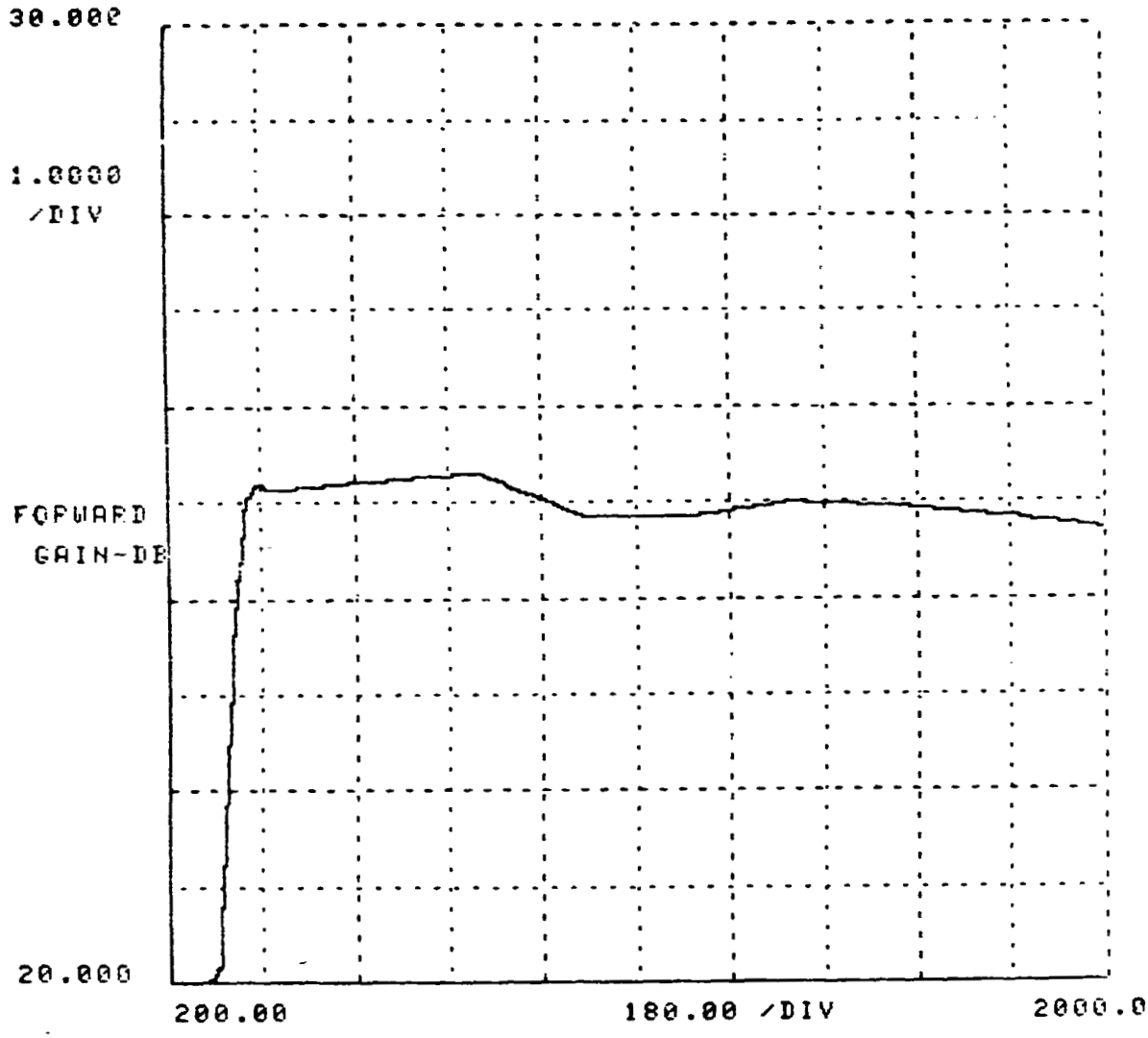

Figure 4-1 Amplifier Gain Measured at 77K.

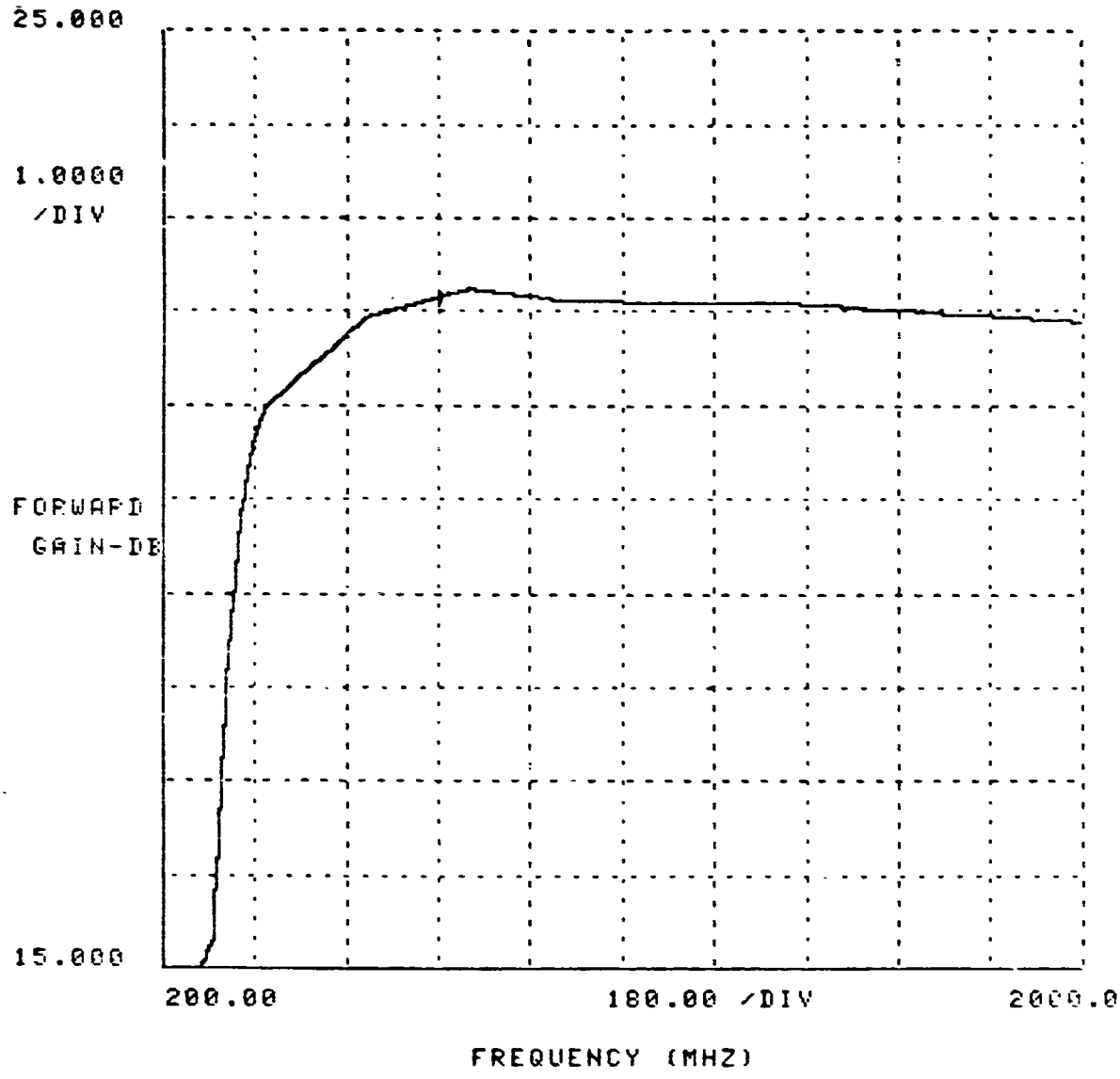

Figure 4-2 Amplifier Gain Measured at 300K.

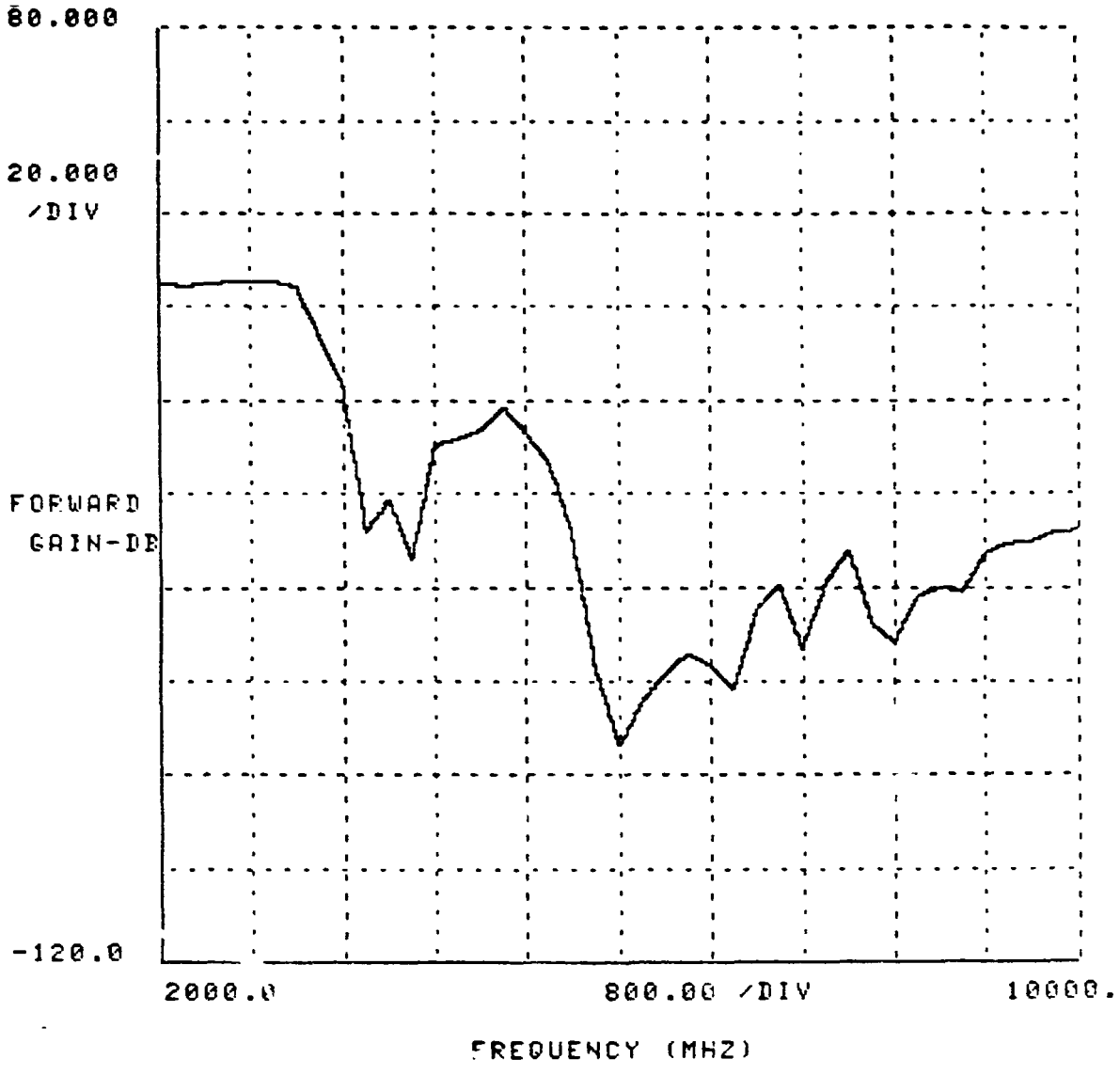

Figure 4-3 Amplifier High Frequency Roll-Off Measured at 77K.

network analyzer; the results of these measurements at 77K are presented in Figure 4-4 and 4-5. The 300K data is almost the same as that shown in Figures 4-4 and 4-5. The forward VSWR was found to be less than 2:1, while the reverse VSWR was less than 2.5:1 over the 200 to 2000 MHz region. The forward and reverse VSWR's remain constant over the 200 MHz to 3200 MHz frequency range and then start to increase at about 3300 MHz.

4.3 Noise Figure

The test set-up shown schematically in Figure 4-6 was used to measure the noise figure of the GaAs FET amplifier at 77K and 300K.[4-1,4-2,4-3] The noise figure was measured at three different frequencies in the 500 MHz to 2000 MHz frequency range, and the results of these measurements are listed in Table 4-1. A 0.007 dB/K decrease in the noise figure was observed as the GaAs FET was cooled from 300K to 77K.

4.4 Gain Compression

The schematic diagram presented in Figure 4-7 shows the experimental arrangement that was used to measure the amplifier's 1 dB gain compression. The signal generator is used to deliver a single frequency, low harmonic continuous wave CW output. With the 10 dB attenuator "in", the output attenuator dial is adjusted to a convenient reference point on the power meter, with the power output approximately 10 dB below the minimum specified compression point. When the 10 dB of attenuation is taken out, the output power will increase. The 1 dB gain compression point is that point where the output power increase is 1 dB less than the increase in input power, i.e., if the input power is increased by 10 dB, the output power will rise only 9 dB. Through an iterative process of varying the input power and

TEMPERATURE (K)	FREQUENCY (MHz)	NOISE FIGURE (dB)
300K	500	3.1
	1250	2.6
	2000	2.9
77K	500	1.6
	1250	1.3
	2000	1.3

TABLE 4-1 SUMMARY OF THE AMPLIFIER NOISE FIGURE MEASUREMENTS

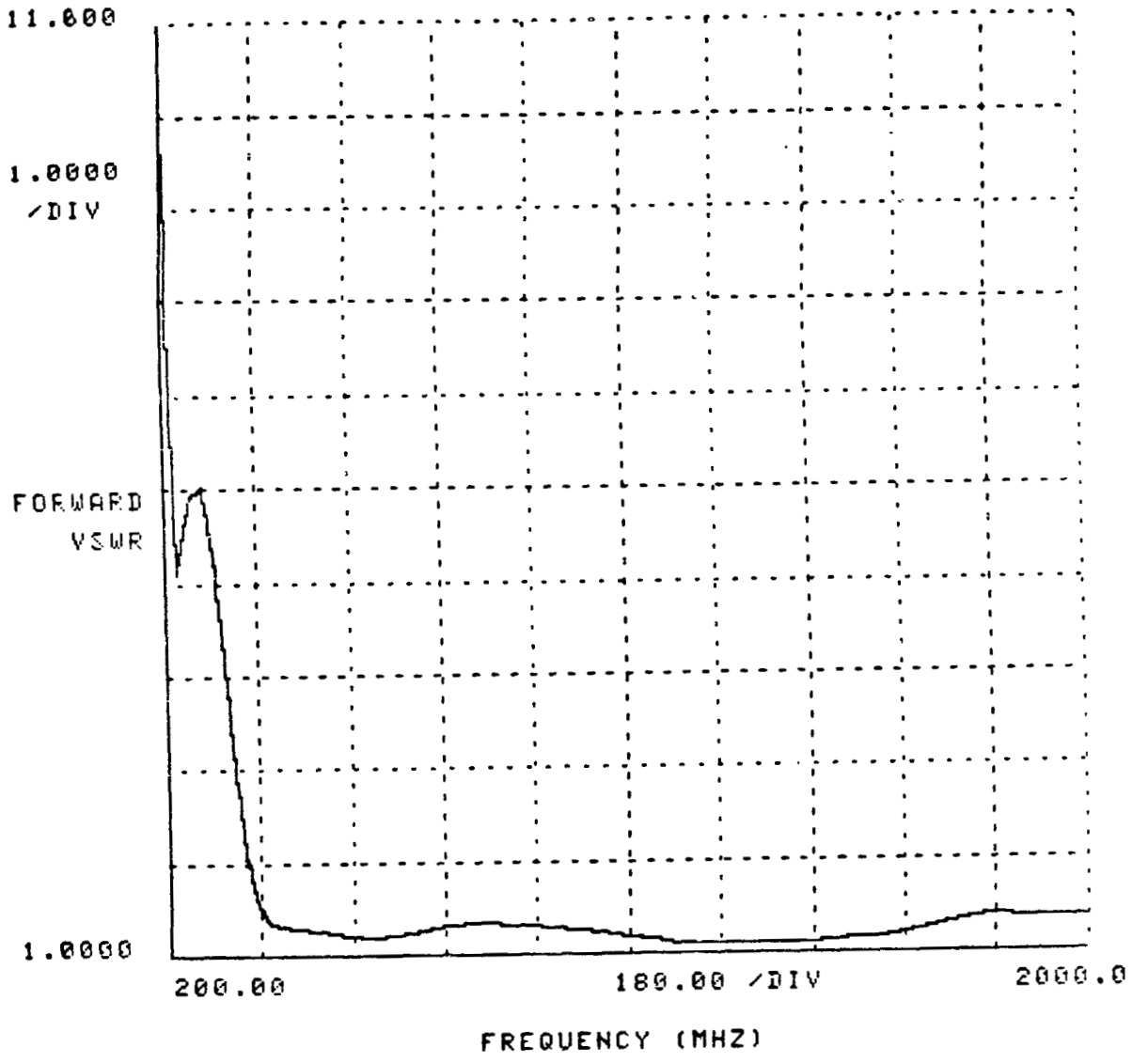

Figure 4-4 Amplifier Forward VSWR Measured at 77K.

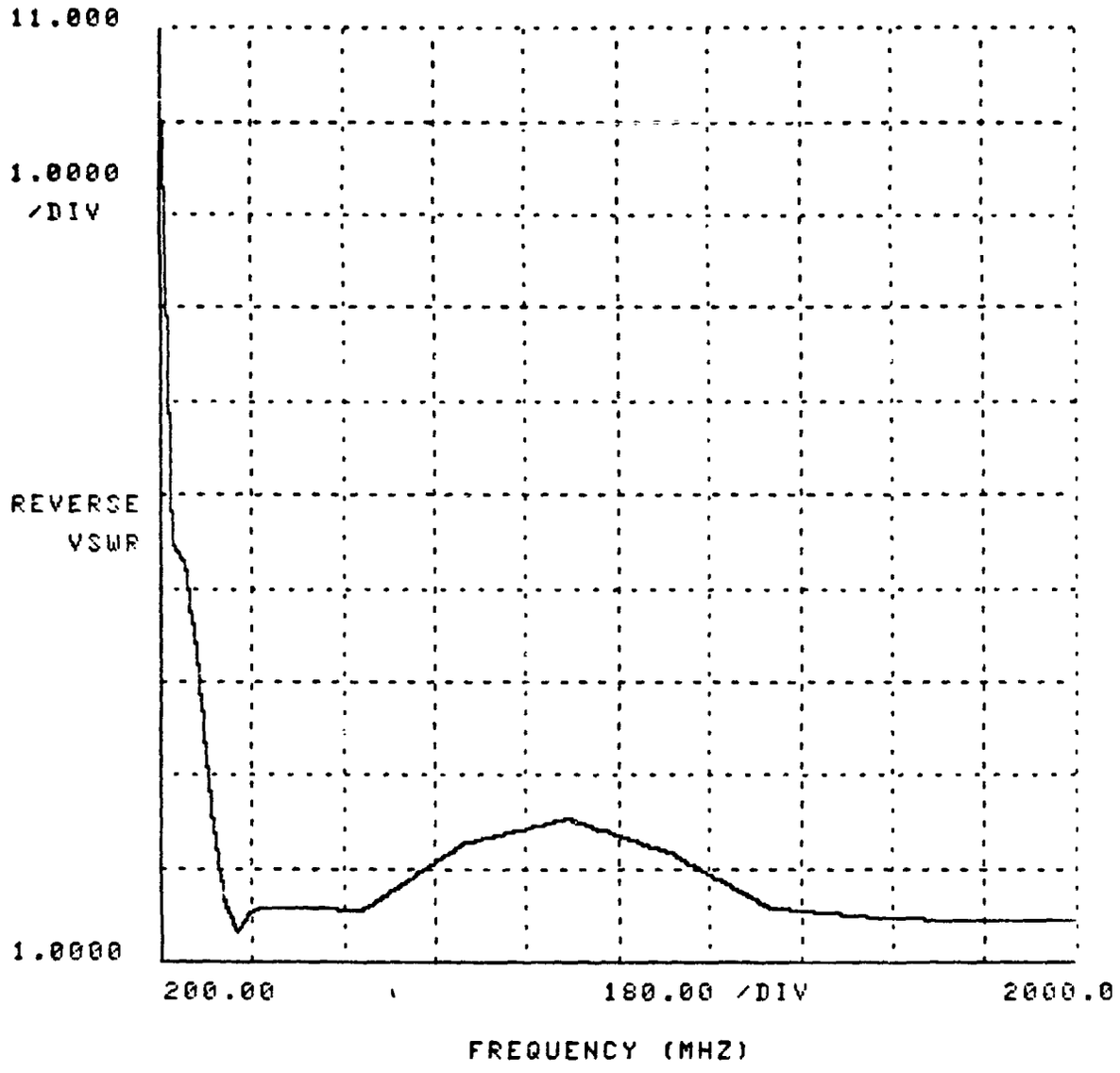

Figure 4-5 Amplifier Reverse VSWR Measured at 77K.

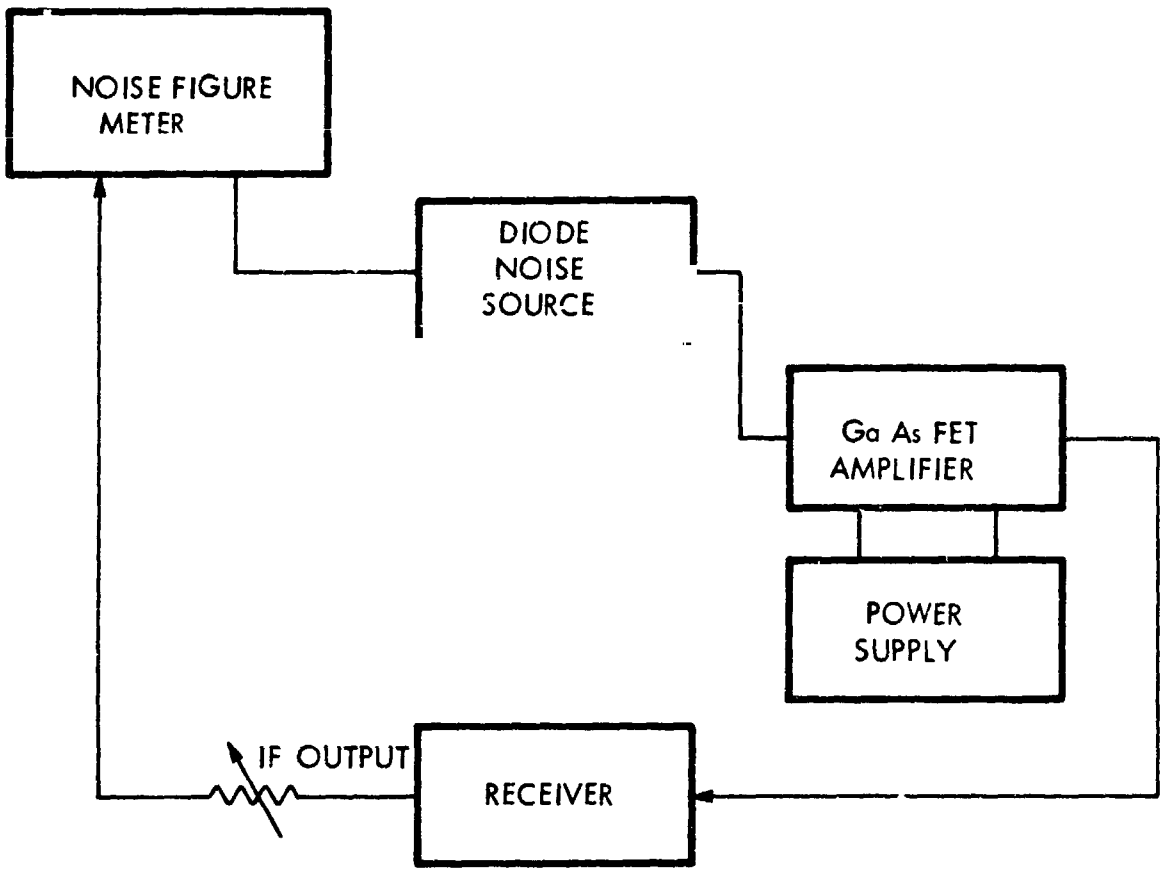

Figure 4-6 Noise Figure Test Set-Up.

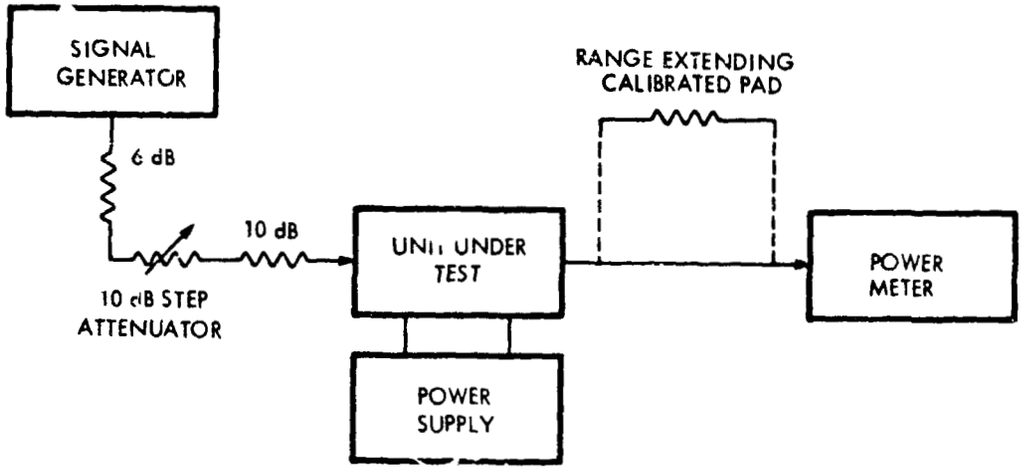

Figure 4-7 1 dB Compression Test Set-Up.

alternating the 10 dB step attenuator in and out, the 1 dB compression point was determined to be +10 dBm at 300K.

No gain compression measurements were made at 77K.

SECTION 5

PHOTODIODE DC CHARACTERIZATION

The DC characteristics of the high frequency Hg_{1-x} Cd .e photodiode, measured at 77K, are presented in this section. The techniques used to measure the photodiode's spectral response, current-voltage characteristic, series resistance, zero bias resistance, detectivity, and quantum efficiency are described, and the experimental data is discussed.

5.1 Spectral Response

A Perkin Elmer 112 Prism Monochrometer with a built-in blackbody source was used to measure the photodiode's spectral response. A graph of the measured relative response versus wavelength is presented in Figure 5-1. The photodiode had a peak spectral response at 12μm, and the cutoff wavelength occurred at approximately 13.1μm. The cutoff wavelength is that wavelength which occurs at 50% of the peak responsivity of the photodiode.

5.2 Current-Voltage Characteristic

The zero bias resistance, series resistance, and the breakdown voltage were all obtained from the photodiode's current-voltage I-V characteristic. A Tektronix Type 576 Curve Tracer was used to measure the photodiode's I-V characteristic shown in the photograph of Figure 5-2.

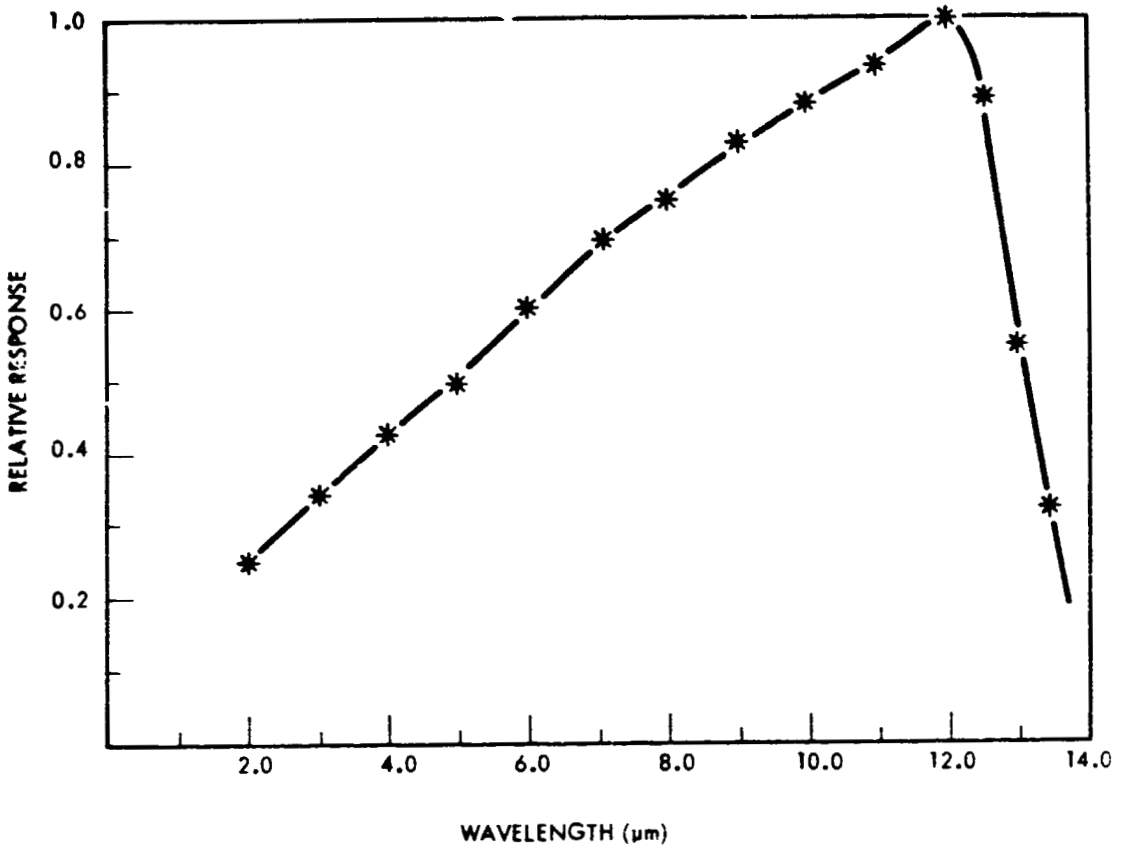

Figure 5-1 Meausred Photodiode Spectral Response.

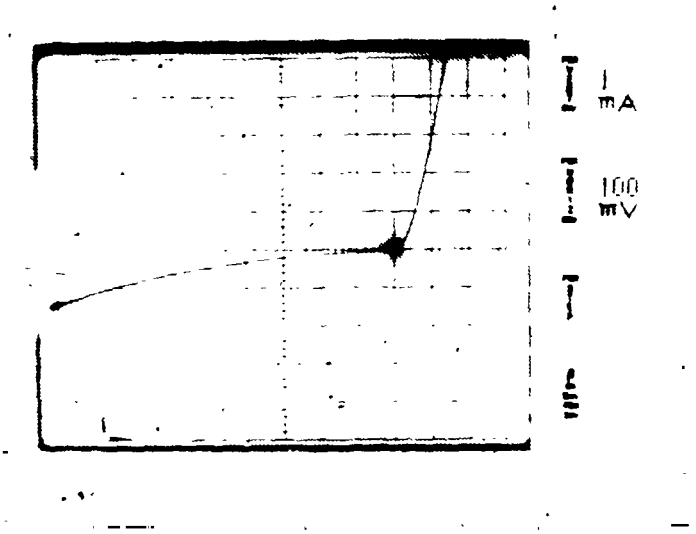

Series Resistance R_S = 20 ohms

Zero Bias Resistance R_O = 1500 ohms

Breakdown Voltage V_B = 1.0 Volts

Peak Wavelength λ_p = 12.0μm

Cutoff Wavelength λ_{co} = 13.1μm

Temperature = 77K

Figure 5-2 I-V Characteristic of the n^+-n^--p $Hg_{1-x}Cd_xTe$ Photodiode

The n^+-n^--p (Hg,Cd)Te photodiode had a series resistance R_S of approximately 20 ohms, and a zero bias resistance R_O of about 1500 ohms. The series resistance was calculated by finding the slope of the forward I-V characteristic, while the zero bias resistance was calculated from the slope of the I-V characteristic at zero bias voltage.

The breakdown voltage was defined to be that voltage which occurs when 1.0mA of excess current flows in the photodiode junction. A breakdown voltage of approixmately 1.0 volt was measured for the n^+-n^--p diode.

5-3 Detectivity

The detectivity D^*_λ of the n^+-n^--p (Hg,Cd)Te photodiode was measured with the detector cooled to a temperature of 77K. The experimental configuration used to measure the D^*_λ is presented in Figure 5-3. A calibrated blackbody cavity was used to establish a known source of energy. The amount of energy leaving the blackbody cavity was defined by using an aperture, whose dimensions were precisely known, placed in front of the cavity. The detector signal voltage S due to the 1000K blackbody was measured, and the noise voltage N due to the detector Johnson noise was also measured. The blackbody detectivity D^*_{BB} was calculated from the equation:[5-1]

$$D^*_{BB} = \frac{S}{N} \sqrt{\frac{AB}{P}}$$

Where A is the detector area, B is the noise bandwidth, and P is the amount of incident blackbody power. The detectivity at the peak detector wavelength $D^*_{\lambda p}$ was found from[5-1,5-2]

$$D^*_{\lambda p} = g\, D^*_{BB}$$

where g is the spectral responsivity factor.

The peak detectivity with λ_p = 12.0μm measured at a chopping frequency of 10 KHz and in a bandwidth of 1 Hz was 1.44×10^{10} cm $Hz^{1/2}/W$. Similarly, a detectivity of 1.29×10^{10} cm $Hz^{1/2}/W$ was measured for incident radiation with a wavelength of 10.6μm.

5.4 Quantum Efficiency

The photodiode quantum efficiency at a wavelength of 10.6μm was found by measuring the current responsivity with a

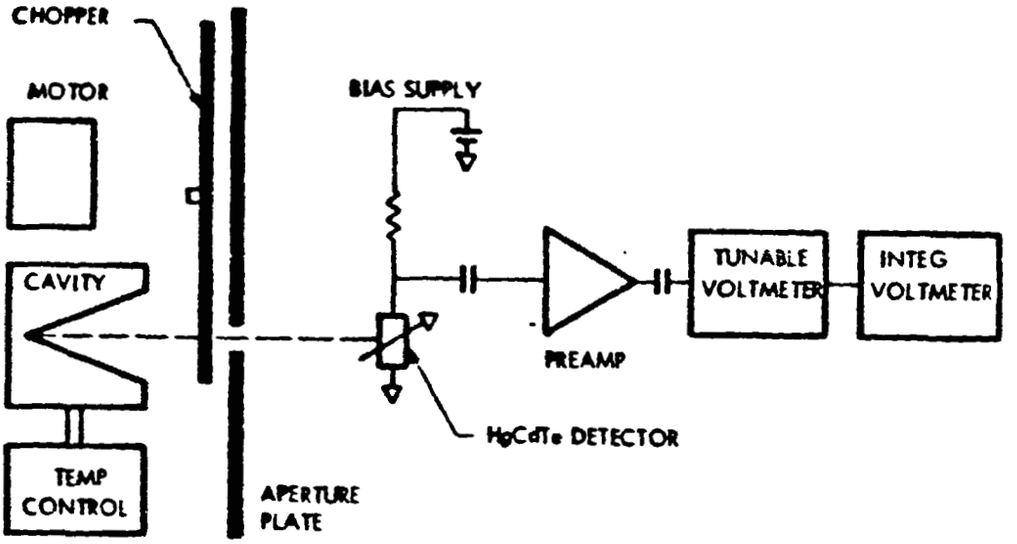

Figure 5-3 Experimental Configuration for Measuring the Photodiode Detectivity.

CO_2 laser beam of calibrated intensity. The laser was focussed onto the photodiode's active area using f/5 optics, and the photoinduced current was measured with a Tektronix 576 Curve Tracer. The incident laser power was continuously monitored during the measurement. The photodiode current responsivity R_m was calculated by dividing the measured photoinduced current by the amount of CO_2 laser power indicent on the photodiode's active area. The quantum efficiency was calculated from

$$\eta = \frac{R_m}{8.53 \text{ (A/W)}}$$

where 8.53 A/W is the current responsivity for an ideal 10.6μm photodiode.

A current responsivity of 5.12 A/W was measured on the n^+-n^--p $Hg_{1-x}Cd_xTe$ photodiode, and the resultant quantum efficiency was calculated to be 60%.

SECTION 6.0

PHOTODIODE/AMPLIFIER CHARACTERIZATION

The heterodyne characteristics of the $Hg_{1-x}Cd_xTe$ photodiode/amplifier combination were measured. The heterodyne measurements included the following:

- Shot noise frequency response,
- Blackbody heterodyne frequency response, and
- Noise equivalent power at 2.0 GHz.

All of the measurements were made in the 100 MHz to 2000 MHz frequency range with the photodiode/amplifier maintained at a temperature of 77K. In addition, the impedance of the photodiode was measured as a function of frequency from 100 MHz to 2000 MHz. The results and techniques used for the heterodyne characterization of the photodiode/amplifier are presented in this section.

6.1 Impedance Characterization

The variation of only the photodiode IF impedance was measured over the frequency range from 100 to 2000 MHz using a computer controlled Hewlett-Packard 8524B network analyzer. Figure 6-1 presents a diagram of the experimental apparatus that was used to perform these measurements. The CO_2 laser was focused onto the photodiode's active area using f/5 optics, and the DC reverse bias voltage was introduced via a bias tee inserted into the coaxial line carrying the RF signal from the network analyzer.

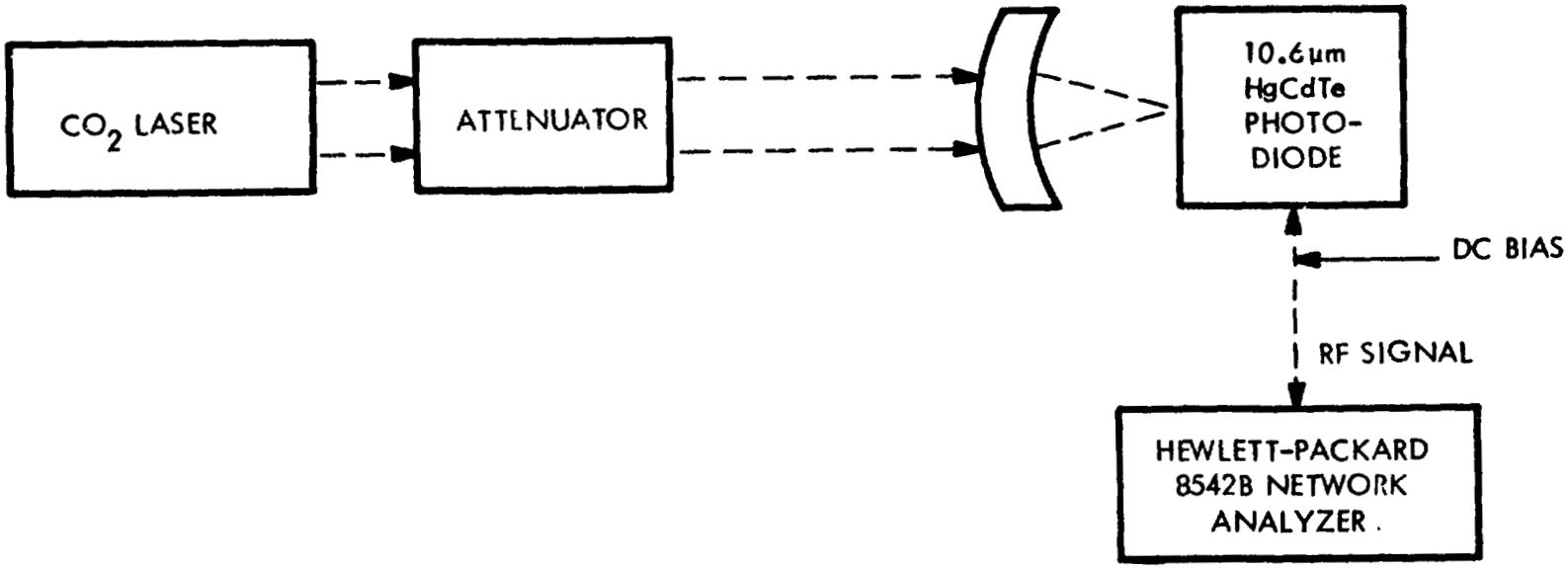

Figure 6-1 Schematic Diagram of the Experimental Configuration for Measuring the Photodiode Impedance.

The impedance measurements were performed with the photodiode cooled to 77K. In addition, the diode impedance data was normalized to exclude any parasitic impedances caused by the transmission line structure, SMA connectors and coaxial cables. The normalization was accomplished by measuring the impedance of the transmission line structure located in the microwave mount shorted to ground. The measurements were made with the mounting structure in the liquid nitrogen dewar. The data was stored in the computer, and subsequent diode impedance measurements were then automatically normalized.

The measured voltage-standing-wave-ratio for the $Hg_{1-x}Cd_xTe$ photodiode is presented in Figure 6-2. The data was taken with the photodiode biased at two different reverse bias voltages, 0.1 and 0.5 volts, and with 0.4 milliwatts of CO_2 laser power incident upon the photodiode. The bias voltages and laser power level chosen for this measurement are typical of those required for obtaining the optimum photodiode heterodyne sensitivity.

The data presented in Figure 6-2 shows that the photodiode's VSWR is close to 2:1 in the 500 to 2000 MHz frequency interval, while at lower frequencies, <500 MHz, the VSWR increases to values greater than 5:1. Therefore, since the diode impedance was nearly 2:1 over the GaAs FET amplifier bandwidth, it was decided that no microwave matching of the amplifier to the photodiode was necessary. Instead, the RF input section of the amplifier was designed to be 50 ohms, and the GaAs FET's were matched to the 50 ohm transmission line structure.

6.2 Blackbody Heterodyne Frequency Response

The heterodyne frequency response and sensitivity (noise equivalent power per unit bandwidth NEP/B or effective heterodyne

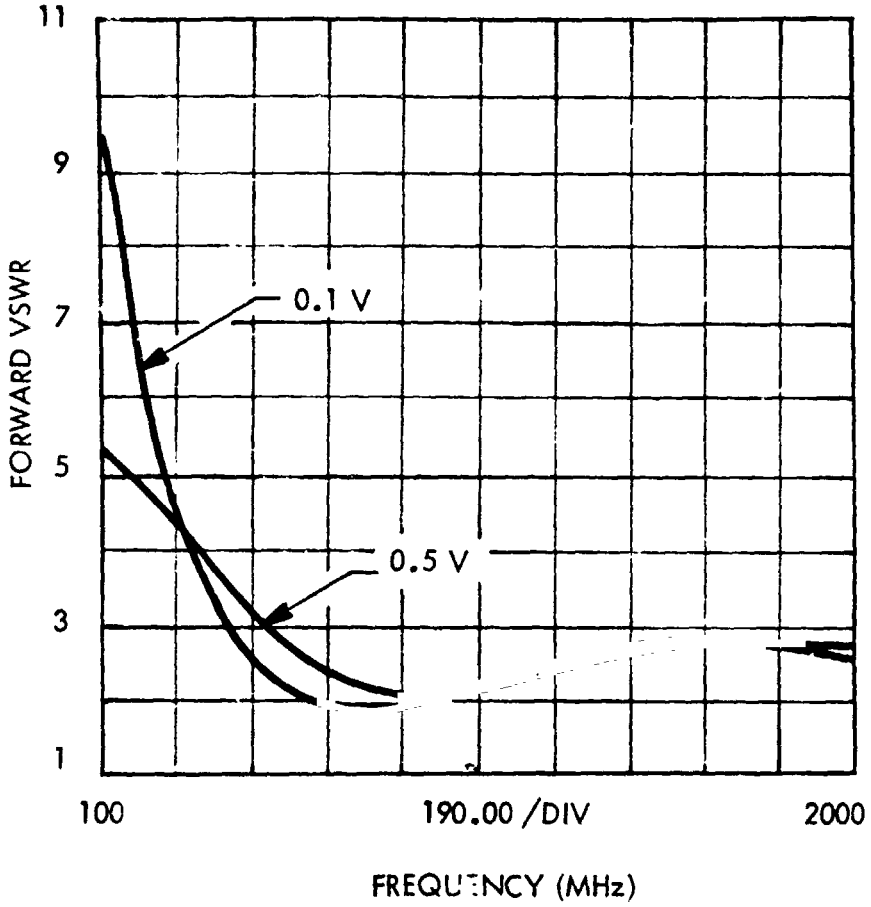

Figure 6-2 VSWR Data for the $Hg_{1-x}Cd_xTe$ Photodiode Illuminated with 0.4 mW of CO_2 Laser Radiation and Reverse Biased with 0.1 and 0.5 volts.

quantum efficiency) was measured by beating a blackbody source (T = 1000 K) against the CO_2 laser local oscillator source.[6-1,6-2,6-3] The local oscillator source power is adjusted so that the shot noise dominates the thermal noise in the receiver. The narrow laser line which is linearly polarized will beat with the spectral components of the blackbody above and below the P(20) local oscillator frequency to provide two side bands which fold into the passband of the IF amplifier.

The diode is made shot noise limited by focusing sufficient laser local oscillator power onto the device's active area to overcome the thermal noise, f/3 optics are used to focus the radiation. The heterodyne frequency spectrum was determined by slowly scanning a spectrum analyzer over the heterodyne signal response, and synchronously detecting the chopped signal by connecting a lock-in amplifier to the vertical output of the spectrum analyzer. The output of the lock-in amplifier and the scan out of the spectrum analyzer are fed into the y and x axis, respectively of an x-y recorder. Figure 6-3 is a diagram illustrating the test setup for measuring the heterodyne frequency response.

Data showing the observed heterodyne frequency response is presented in Figure 6-4. The heterodyne frequency response was found to be fairly flat in the 300 MHz to 2000 MHz frequency range for incident CO_2 laser power levels of 0.390 milliwatts and at a reverse bias voltage of 1.22 volts., No data was taken above 2000 MHz because of the lack of a spectrum analyzer with a bandwidth greater than 2000 MHz.

6.3 Shot Noise Frequency Response

The shot noise frequency response was measured using a technique which is very similar to the heterodyne frequency

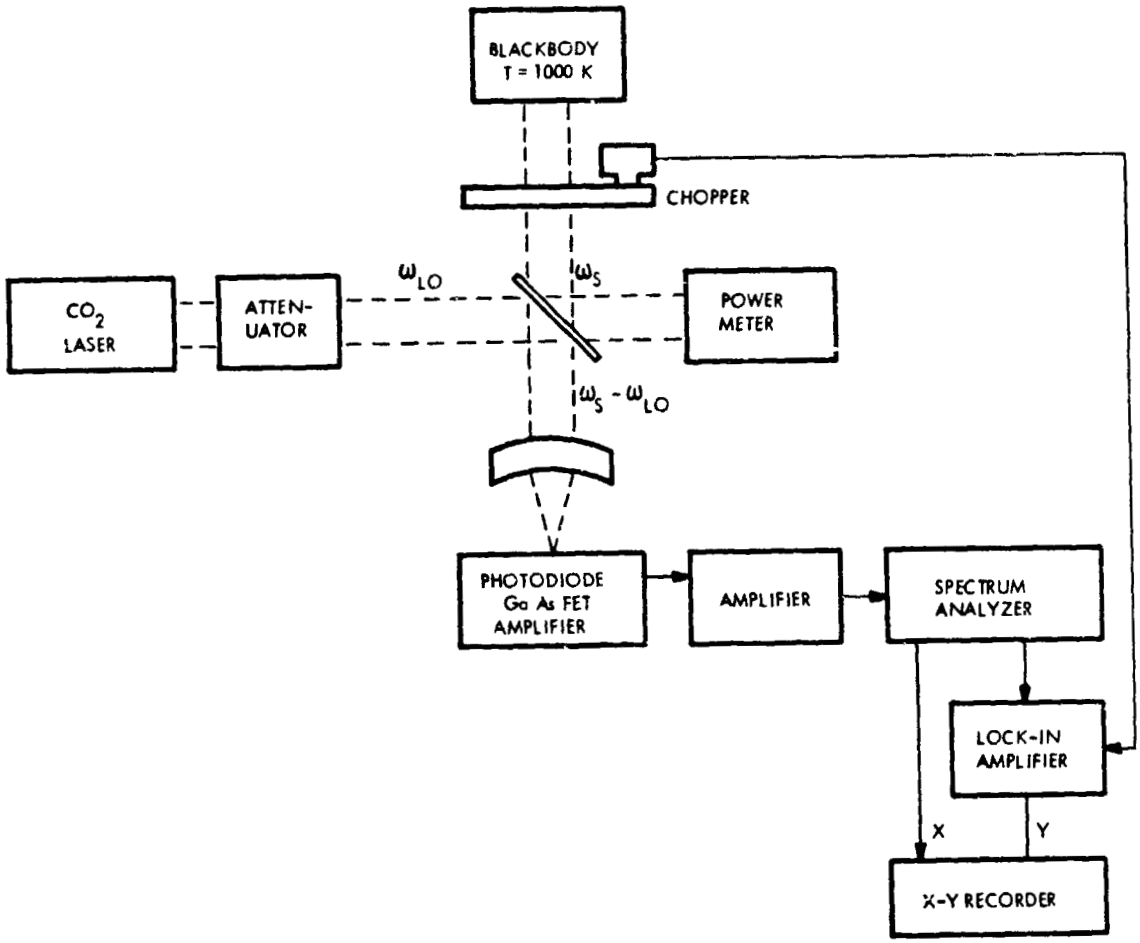

Figure 6-3 Test Set-Up for the Heterodyne Frequency Response Measurement.

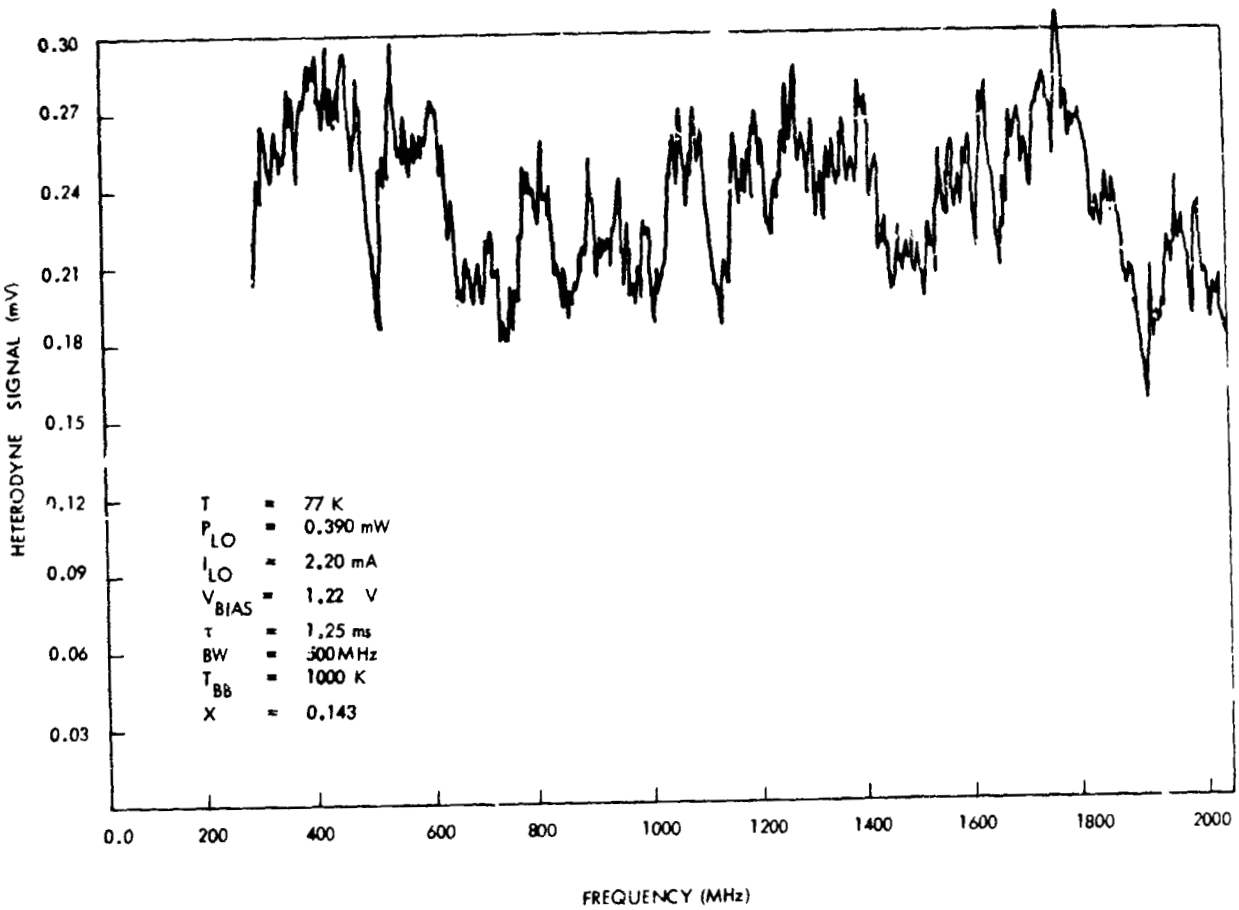

Figure 6-4 Measured Heterodyne Frequency Response of the $Hg_{1-x}Cd_xTe$ Photodiode.

response measurement illustrated in Figure 6-3.[6-1,6-3] The difference in the two methods is that the shot noise does not utilize a blackbody, the CO_2 laser beam is chopped, and the signal induced in the photodiode, i.e., the shot noise is synchronously detected. The observed shot noise frequency response was very similar to that of the heterodyne response presented in Figure 6-4.

The shot noise was also found to be flat in the 300 MHz to 2000 MHz frequency range for a reverse bias voltage of 1.22 volts and an incident CO_2 laser power level of 0.390 milliwatts.

6-4 Blackbody Heterodyne NEP/B

The heterodyne sensitivity, or noise equivalent power per unit bandwidth was measured by beating a blackbody source (T = 1000K) against the CO_2 laser local oscillator source.[6-1,6-2,6-3] The local oscillator source power was adjusted so that the shot noise dominated the thermal noise in the receiver.

The broadband output of the amplifier was fed into a tunable RF bandpass filter, which was used to perform heterodyne measurements in the 300 MHz to 2000 MHz frequency region. The upper cutoff frequency of 2000 MHz was due to the second stage cascaded amplifier with a bandwidth of 10 MHz to 2000 MHz, and gain of 40 dB. The cascaded amplifier was necessary in order to obtain a measurable signal-to-noise ratio. Otherwise, these measurements could have been made using the bandwidth of the GaAs FET amplifier. The output of the bandpass filter was then fed into a crystal detector. The signal-to-noise ratio was measured by a synchronous detection scheme, in which the output of the crystal detector and the blackbody chopper frequency were

simultaneously fed into a lock-in amplifier that contained the signal-to-noise ratio option. A schematic diagram illustrating the blackbody heterodyne radiometry technique is presented in Figure 6-5.[6-1]

The NEP/B was found by measuring the signal-to-noise ratio (S/N) and using the expression[6-1,6-2,6-3]

$$NEP/B = 2\left(\frac{S}{N}\right)^{-1} h\nu\,(B\tau)^{\frac{1}{2}} K \left\{ \frac{\varepsilon_{BB}}{\exp\,(h\nu/kT_{BB}) - 1} - \frac{\varepsilon_{BB}}{\exp\,(h\nu/kT_{R}) - 1} \right\} \quad (6\text{-}1)$$

where τ is the post-detection integration time, B is the IF bandwidth, K is the optics transmission and chopper factor, T_{BB} and T_R are the blackbody and room temperatures, and ε_{BB} and ε_R are the emissivities of the blackbody and room temperatures.

The NEP/B was found to be approximately flat, i.e., within about 20%, over the frequency range of 300 MHz to 2000 MHz. More specifically, at 2000 MHz the following heterodyne parameters were measured for a reverse bias voltage of 0.928 volts, and an incident laser power of 0.653 mW.:

Signal S:	62 μV
Noise N:	0.7 μV
IF Frequency:	2000 MHz
IF Bandwidth B:	100 MHz
Integration Time:	400 msec
Transmission and Chopper Factor K:	0.143

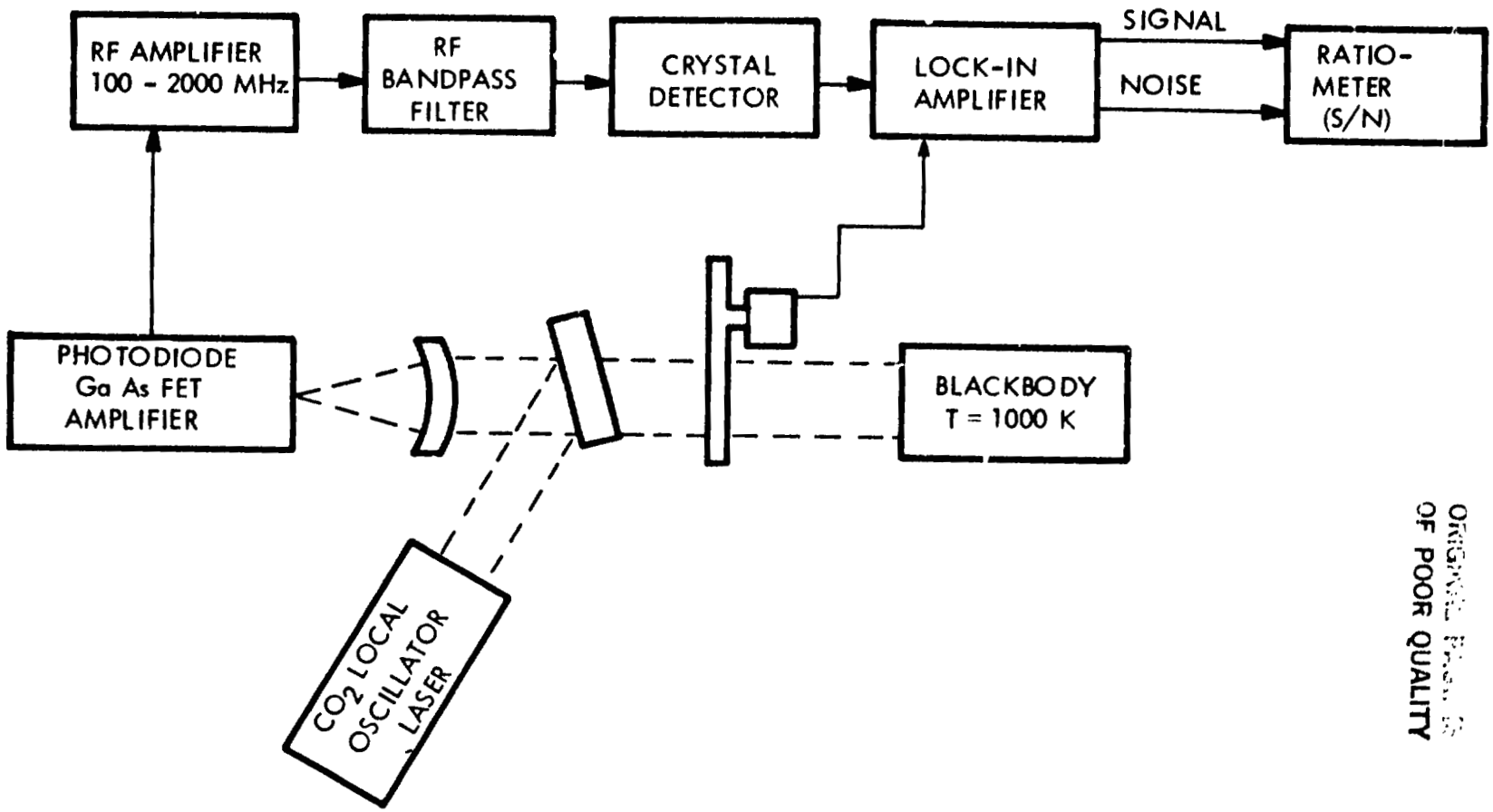

Figure 6-5 Blackbody Heterodyne Radiometer.

Using these parameters a NEP/B of 5.7×10^{-20}W/Hz was found from Equation 6-1. The resulting effective heterodyne quantum efficiency was 32.8% at 2.0 GHz.

SECTION 7

CONCLUSIONS AND RECOMMENDATIONS

A HgCdTe photodiode/GaAs FET amplifier package was designed and fabricated to have an NEP/B of 5.7×10^{-20} W/Hz at 77K. The technology for designing and building a low noise GaAs FET amplifier with a gain of 25 dB, noise figure of 1.6 dB, bandwidth of 300 MHz to 3200 MHz, and operating at 77K was successfully developed during the program.

The photodiode/amplifier packaged was housed in a specially designed liquid nitrogen dewar in which both the photodiode and amplifier are each maintained at a temperature of 77K. The voltage regulator used to power the amplifier is contained in a separate package which is mounted on the dewar wall. The regulator package is at a temperature somewhere in the range from 200K to 300K; this is sufficient to ensure that carrier freeze out does not occur in the silicon devices used in the regulator circuit. The DC bias T used to apply a reverse bias voltage to the diode is also contained in a separate package.

There are several recommendations for improving the performance of the photodiode/amplifier package. These recommendations are:

1. Reduce the complexity of the GaAs amplifier, voltage regulator, and DC bias T packages by designing each of these items into a single amplifier/regulator/bias T package. This will also help reduce the VSWR caused by all the electrical connections to the separate packages.

2. Design a voltage regulator that can operate at 77K.

3. Utilize an anti-reflection coating for 8-14μm radiation on the diode's photoactive region in order to increase the effective heterodyne quantum efficiency.

4. Investigate methods for reducing the GaAs amplifier's lower cutoff frequency to 10 MHz. Currently, the 300 MHz frequency is due to the large 1/f noise which occurs in GaAs FET's below this frequency.

SECTION 8

REFERENCES

SECTION 1

1-1 J.F. Shanley and L.C. Perry, IEEE International Electron Devices Meeting Technical Digest, 424, (1980).

1-2 J.F. Shanley, C.T. Flanagan, J.A. Mroczkowski, M.B. Reine, and T.N. Casselman, Heterodyne Laser Mixer Detector Study, Air Force Wright Aeronautical Laboratory, Contract Number F33615-79-C-1762, WPAFB, Ohio 45433

1-3 A. Betz, Proceedings of the Heterodyne Systems and Technology Conference, Williamsburg, VA, NASA Publication 2138, 11, (1980).

SECTION 2

2-1 J.F. Shanley, and C.T. Flanagan, Heterodyne Systems Technology Conference, Williamsburg, VA, 25-27 March 1980.

2-2 J.F. Shanley and L.C. Perry, IEEE Int. Electron Device Meeting Tech. Digest, 424 (1978).

2-3 J.L. Schmit and E.L. Stelzer, J. Electron Mater. 7, 65 (1978).

2-4 H.R. Huff, J. Knaus, and B.H. Bneazeale, Proc. of the IRIS Specialty Group on IR Detectors (1974).

2-5 B.I. Boltaks, Diffusion in Semiconductors, Academic Press, New York, 93 (1963).

2-6 M.D. Blue, Proceedings of the International Conference on Semiconductor Physics 1, Academic Press, New York, 233-237 (1964).

SECTION 3

3-1 S. Weinreb, IEEE Transactions on Microwave Theory anbd Techniques, Vol. MTT 28, No. 10, 1041 (1980).

3-2 D. Williams, S. Beinreb, and W. Lum, Microwave J. Vol. 23, No. 10, 73, October 1980.

3-3 C.A. Liechti and R.A. Larrick, IEEE Transaction on Microwave Theory and Techniques, Vol. MTT-24, 376-381, (1976).

3-4 E.J. Fjarlie, Applied Optics, Vol. 16, No. 2, 385-392, (1977).

SECTION 4

4-1 H.J. Reich, J.K. Skalnik, P.F. Ordung, and H.L. Krauss, Microwave Principles, D. Van Nostrand, Inc., Princeton, NJ, (1957).

4-2 R.E. Collin, Foundations for Microwave Engineering, McGraw-Hill Book Company, New York, (1966).

4-3 J.D. Krauss, Radio Astronomy, McGraw Hill Book Comp[any, New York, (1966).

SECTION 5

5-2 D. Long (1977), "Photovoltaic and Photoconductive Infrared Detectors," Topics in Applied Physics, Vol 19: Optical and Infrared Detectors, Springer-Verlag, Berling, 110-112.

5-2 P.W. Kruse, L.D. McGlauchlin, R.B. McQuistan (1962), Elements of Infrared Technology, Wiley and Sons, New York.

SECTION 6

6-1 J.F. Shanley and L.C. Perry (1978), IEEE Int. Electron Device Meeting Tech. Digest, 424.

6-2 D.L. Spears (1975), "Planar HgCdTe Quadrantal Heterodyne Arrays with GHz Response at 10.6 m," in Proc. of IRIS Detector Specialty Group Meeting, Fort Monmouth, NJ.

6-3 B.J. Peyton, A.J. DiNardo, G.M. Kanischak, F.R. Arams, R.A. Lange, and E.W. Sard, IEEE J. Quant. Electron. QE-8, 2, 252-263 (1972).